Bulk Transfer Coefficients Estimated from Eddy-Covariance Measurements over Lakes and Reservoirs

Sofya Guseva[1], Fernando Armani[2], Ankur Rashmikant Desai[3], Nelson Luís Dias[4], Thomas Friborg[5], Hiroki Iwata[6], Joachim Jansen[7], Gabriella Lükő[8], Ivan Mammarella[9], Irina Repina[10], Anna Rutgersson[7], Torsten Sachs[11], Katharina Scholz[12], Uwe Spank[13], Victor M Stepanenko[14], Péter Torma[8], Timo Vesala[15], and Andreas Lorke[16]

[1]University Koblenz-Landau (Landau)
[2]Universidade Federal do Paraná
[3]University of Wisconsin-Madison
[4]Federal University of Paraná
[5]University of Copenhagen
[6]Shinshu University
[7]Uppsala University
[8]Budapest University of Technology and Economics
[9]University of Helsinki
[10]A.M. Obukhov Institute of Atmospheric Physics
[11]GFZ German Research Centre for Geosciences
[12]University of Innsbruck
[13]Technical University of Dresden
[14]Lomonosov Moscow State University
[15]University of Helsinki, Institute for Atmospheric and Earth System Research
[16]University of Koblenz and Landau

November 22, 2022

Abstract

The drag coefficient (CDN), Stanton number (CHN) and Dalton number (CEN) are of particular importance for the bulk estimation of the surface turbulent fluxes of momentum, heat and water vapor at water surfaces. Although these bulk transfer coefficients have been extensively studied over the past several decades mainly in marine and large-lake environments, there are no studies focusing on their synthesis for many lakes. Here, we evaluated these coefficients through directly measured surface fluxes using the eddy-covariance technique over more than 30 lakes and reservoirs of different sizes and depths. Our analysis showed that generally CDN, CHN, CEN (adjusted to neutral atmospheric stability) were within the range reported in previous studies for large lakes and oceans. CHN was found to be on average a factor of 1.4 higher than CEN for all wind speeds, therefore, likely affecting the Bowen ratio method used for lake evaporation measurements. All bulk transfer coefficients exhibit substantial increase at low wind speeds ($<$ 3 m s-1), which could not be explained by any of the existing physical approaches. However, the wind gustiness could partially explain this increase. At high wind speeds CDN, CHN, CEN remained relatively constant at values of 2 10-3, 1.5 10-3, 1.1 10 -3, respectively. We found that the variability of the transfer coefficients among the lakes could be associated with lake surface area or wind fetch. The empirical formula C=b1[1+b2exp(b3 U10)] described the dependence of CDN, CHN, CEN on wind speed well and it could be beneficial for modeling when coupling atmosphere and lakes.

Hosted file

essoar.10511514.1.docx available at https://authorea.com/users/537454/articles/599338-bulk-transfer-coefficients-estimated-from-eddy-covariance-measurements-over-lakes-and-reservoirs

S. Guseva[1], F. Armani[2], A. R. Desai[3], N. L. Dias[4], T. Friborg[5], H. Iwata[6], J. Jansen[7,8], G. Lükő[9], I. Mammarella[10], I. Repina[11,12], A. Rutgersson[13], T. Sachs[14], K. Scholz[15], U. Spank[16], V. Stepanenko[12,17,18], P. Torma[9], T. Vesala[10,19], and A. Lorke[1]

[1] Institute for Environmental Sciences, University of Koblenz-Landau, Landau, Germany.

[2] Federal University of Paraná, Curitiba, PR, Brasil.

[3] Department of Atmospheric and Oceanic Sciences, University of Wisconsin-Madison, Madison, WI, USA.

[4] Department of Environmental Engineering, Federal University of Paraná, Curitiba, PR, Brasil.

[5] Department of Geosciences and Natural Resource Management, Oester Voldgade 10, 1350 Copenhagen K, Denmark.

[6] Department of Environmental Science, Faculty of Science, Shinshu University, Matsumoto, Japan.

[7] Department of Ecology and Genetics / Limnology, Uppsala University, Uppsala, Sweden.

[8] Département des Sciences Biologiques, Groupe de Recherche Interuniversitaire en Limnologie, Université du Québec à Montréal, Montréal, QC, Canada.

[9] Department of Hydraulic and Water Resources Engineering, Budapest University of Technology and Economics, Budapest, Hungary.

[10] Institute for Atmospheric and Earth System Research/Physics, Faculty of Science, University of Helsinki, Helsinki, Finland.

[11] A.M. Obukhov Institute of Atmospheric Physics, Moscow, Russia.

[12] Research Computing Center, Lomonosov Moscow State University, Moscow, Russia.

[13] Department of Earth Sciences, Uppsala University, Uppsala, Sweden.

[14] GFZ German Research Centre for Geosciences, Potsdam, Germany.

[15] Department of Ecology, University of Innsbruck, Innsbruck, Austria.

[16] Technische Universität Dresden, Faculty of Environmental Sciences, Institute of Hydrology and Meteorology, Chair of Meteorology, PF 1117, 01735 Tharandt, Germany.

[17] Faculty of Geography, Lomonosov Moscow State University, Moscow, Russia.

[18] Moscow Center of Fundamental and Applied Mathematics, Moscow, Russia.

[19] Institute for Atmospheric and Earth System Research/Forest Sciences, Faculty of Agriculture and Forestry, University of Helsinki, Finland.

Corresponding author: Sofya Guseva (guseva@uni-landau.de)

Key Points:

- The bulk transfer coefficients exhibit a substantial increase at low wind speeds in lakes which could partially be associated with gusts
- Average drag coefficients significantly correlated with lake surface area at winds exceeding 3 m s^{-1}
- An empirical function describing the dependence of the transfer coefficients on wind speed could be beneficial when modeling lakes

Abstract

The drag coefficient (C_{DN}), Stanton number (C_{HN}) and Dalton number (C_{EN}) are of particular importance for the bulk estimation of the surface turbulent fluxes of momentum, heat and water vapor at water surfaces. Although these bulk transfer coefficients have been extensively studied over the past several decades mainly in marine and large-lake environments, there are no studies focusing on their synthesis for many lakes. Here, we evaluated these coefficients through directly measured surface fluxes using the eddy-covariance technique over more than 30 lakes and reservoirs of different sizes and depths. Our analysis showed that generally C_{DN}, C_{HN}, C_{EN} (adjusted to neutral atmospheric stability) were within the range reported in previous studies for large lakes and oceans. C_{HN} was found to be on average a factor of 1.4 higher than C_{EN} for all wind speeds, therefore, likely affecting the Bowen ratio method used for lake evaporation measurements. All bulk transfer coefficients exhibit substantial increase at low wind speeds (< 3 m s^{-1}), which could not be explained by any of the existing physical approaches. However, the wind gustiness could partially explain this increase. At high wind speeds, C_{DN}, C_{HN}, C_{EN} remained relatively constant at values of $2 \cdot 10^{-3}$, $1.5 \cdot 10^{-3}$, $1.1 \cdot 10^{-3}$, respectively. We found that the variability of the transfer coefficients among the lakes could be associated with lake surface area or wind fetch. The empirical formula $C = b_1 \left[1 + b_2 \exp(b_3 U_{10})\right]$ described the dependence of C_{DN}, C_{HN}, C_{EN} on wind speed well and it could be beneficial for modeling when coupling atmosphere and lakes.

1 Introduction

The major process that governs the interaction between the atmosphere and surface waters is the turbulent exchange of momentum, heat and gases at the air-water interface. Although lakes and reservoirs occupy only about 3% of the land surface area (Downing et al., 2006), they are known to have an impact on local weather and climate. For example, lakes affect the stability of the atmosphere above (Sun et al., 1997), leading to the formation of clouds and precipitation on the shores (Changnon & Jones, 1972; Kato & Takahashi, 1981; Eerola et al., 2014; Thiery et al., 2016). Furthermore, lakes and reservoirs are recognized as significant contributors to the global carbon cycle by emitting significant amounts of carbon dioxide and methane (DelSontro et al., 2018; Rosentreter et al., 2021).

The past three decades have seen a rapid development of lake models (Stepanenko et al., 2014) and their incorporation into numerical weather and climate prediction models (Ljungemyr et al., 1996; Salgado & Le Mogne, 2010; Mironov et al., 2010). Experiments on the coupling of lakes and the atmospheric model revealed their beneficial impact on the weather prediction quality (Balsamo et al., 2012). A number of case studies have demonstrated the importance of lakes for extreme local weather phenomena, such as lake-effect snow over Great American lakes (Fujisaki-Manome et al., 2020), deep hazardous convection over Great African lakes (Thiery et al., 2016), wind speeds over Lake Superior (Desai et al., 2009), or stratiform cloudiness in winter over Lake Ladoga (Eerola et al., 2014). Thus, an accurate representation of the exchange of momentum, heat and water vapor at the air-water interface in water bodies is essential.

In state-of-the-art, momentum, sensible and latent heat fluxes are usually determined based on gradient approaches utilizing transfer coefficients (bulk transfer coefficients) and easy to measure meteorological and limnological variables, i.e., wind speed, air temperature, air humidity and water surface temperature (Stull, 1988). The exchange at the air-water interface and therewith the bulk coefficients are controlled by the boundary-layer turbulence. The bulk exchange coefficient of momentum, known as the drag coefficient ($C_D,\ C_{\mathrm{DN}}$) (Garratt, 1977), is of particular importance for all air-water fluxes. The coefficients of heat ($C_H,\ C_{\mathrm{HN}}$) and water vapor exchange ($C_E,\ C_{\mathrm{EN}}$) are also known as Stanton and Dalton numbers, respectively. Here, "N" stands for "neutral" transfer coefficients, corresponding to the neutral thermal stability of the atmosphere. The transfer coefficients depend on the measurement height of the mean wind speed, air temperature and humidity, respectively, and for this reason, they are usually reported for the reference meteorological height of 10 m.

A considerable amount of studies has been published on the momentum flux and the drag coefficient starting from the early 1950s when the fundamental work, presenting the theory later on named as Monin-Obukhov similarity theory, was published (Monin & Obukhov, 1954; Obukhov, 1971). The theory aims at describing the structure of turbulence in the atmospheric surface layer about several tens of meters thick with the assumption of the fluxes being constant and independent of height. Similarity laws introduce functional relations to derive the universal shapes for the vertical profiles of different quantities for atmospheric thermal stability other than neutral. During the past decades, considerable effort has been devoted to define the exact form of these similarity functions (Paulson, 1970; Businger et al., 1971; Högström, 1988; Zilitinkevich & Calanca, 2010).

As the drag coefficient is one of the key parameters in atmospheric and lake models, the errors in its parameterization lead to errors in the bulk flux estimates. Therefore, numerous early studies focused on exploring different parameterizations of the drag coefficient over the land and oceans in terms of wind speed, atmospheric stability, and surface roughness, which could be a function of the surface wave field (for oceans) (Garratt, 1977; Kantha & Clayson, 2000).

Most of the extensive field measurement campaigns over the oceans have been conducted during the last 30 years of the 20th century (Large & Pond, 1981; Godfrey & Beljaars, 1991; Smith et al., 1996; Fairall et al., 1996). Several of these studies agreed that the drag coefficient linearly increases with increasing wind speed ignoring the state of the wave field. More recent parameterizations of the drag coefficient (e.g., the COARE algorithm, (Edson et al., 2013)), however, include a wave dependence. There is still an ongoing scientific discussion concerning the importance of waves and how their impact could be included in the models (Wu et al., 2019).

Along with the studies in the marine environment, the research started to focus on the drag coefficient estimated from measurements over large and medium-sized lakes (e.g., Hicks, 1972; Donelan, 1982; Graf et al., 1984; Simon, 1997). To date, in total, about two dozen studies focusing on lakes have been published since the beginning of the 1970s. In reviewing these studies below, we separated them by the wind speed regime they were interested in. It is usually assumed that surface wave development starts when the wind speed exceeds 3-4 m s^{-1} (Ataktürk & Katsaros, 1999; Kantha & Clayson, 2000). This is also supported by wave measurements in several lakes (Simon, 1997; Guseva et al., 2021). Therefore, we intend to separate the two wind speed regimes using this threshold.

At the "high" wind speed regime (wind speed exceeds 3 m s^{-1}), in the most simplified way, the surface waves are assumed to be fully developed, and the surface roughness length is described as a function of wind stress, which is commonly known as Charnock relationship (Charnock, 1955). However, this assumption might not hold for lakes with limited wind fetch (Donelan, 1990; Geernaert, 1990). Thus, some research has been made to study the drag coefficient as a function of the surface wave state, for example, taking into account wave characteristics such as the wave age (Donelan, 1982; Ataktürk & Katsaros, 1999). Vickers & Mahrt (1997) reported that for a given wind speed the drag coefficient tends to be larger for younger steeper waves representative of short wind fetches than for longer fetches. Ataktürk & Katsaros (1999) could significantly reduce the scatter in the estimated drag coefficients by considering waves in the parameterization of the surface roughness length. However, these studies mainly examined large lakes and only a few were performed in lakes with short fetch and young wave states (Babanin & Makin, 2008; Lükő et al., 2020). Given the fact that the surface wave measurements in lakes are not often available, their effect still could be investigated via analyzing the relationship between the drag coefficient and fetch length.

At the "low" wind speed regime, several studies found that the neutral drag coefficient in lakes and oceans tended to increase by an approximate factor of two up to ten compared to the value of $1.3 \cdot 10^{-3}$ (corresponding to a typical value of open water surface roughness (Foken, 2008)) (Wüest & Lorke, 2003; Woolway et al., 2017). Although the wind speed dependence is obvious, many numerical and empirical studies employ a constant value for the drag coefficient,

which is often considered as a model tuning parameter (Stepanenko et al., 2014). Despite the fact that there have been many attempts to address the reasons of such increase, there is still no consensus in the scientific community. The low wind speed regime was first described as the aerodynamically smooth flow, when the surface waves are buried within the viscous sublayer and the surface roughness is described as a function of the thickness of this layer (Schlichting, 1968). On the contrary, Wu (1988) proposed that the flow is aerodynamically rough and that capillary gravity waves play a key role at low wind speeds. Surface roughness length was described as a function of the water surface tension. As an additional reason for the increase of the drag coefficient at low wind speed, Godfrey & Beljaars (1991) and Grachev et al. (1998) considered the concept of gustiness, which assumes that at "zero" wind speeds there are dry random convective motions – gusts – in the convective boundary layer (CBL). Thus, the "traditional" formulation of the drag coefficient has been modified using the scalar-averaged wind speed (not the vector-averaged wind speed) to account for gusts. All the possible mechanisms mentioned above were addressed in the recent work by Wei et al. (2016). They concluded that none of them explained the increase of the drag coefficient at low wind speeds. However, they found it can be explained by the increase in the turbulent kinetic energy and enhanced buoyant energy. Similar to (Grachev et al., 1998), Sahlée et al. (2014) and Liu et al. (2020) related the increase of the drag coefficient with nonlocal effects, such as the penetration of large convective eddies into the surface layer from the atmosphere above. Liu et al. (2020) introduced the factor describing this effect and estimated it from two-level measurements of wind speed (however, over the land surface and only for neutral conditions). Another formulation of the drag coefficient at low wind speeds was done by Zhu & Furst (2013) relating the drag coefficient to the turbulent kinetic energy budget. However, their fitting coefficients for the drag coefficient formula were found to be site-specific (Liu et al., 2020).

Other studies on the bulk transfer coefficients in lakes branched off from the main direction – potential physical mechanisms – with a focus on the possible correlation between the bulk transfer coefficients and some lake characteristics. Among them are lake depth at the measurement location (Panin et al., 2006), lake surface area (Read et al., 2012; Woolway et al., 2017), wind fetch at the measurement location (Lükő et al., 2020) and lake biota, e.g, submerged macrophytes (Xiao et al., 2013). All studies showed a strong dependence of the transfer coefficients on these lake characteristics. The drag coefficient tends to decrease with increasing water depth, lake area, fetch and in the presence of water plants at the water surface. It is important to note that although Panin et al. (2006) and Woolway et al. (2017) revealed the correlation between the transfer coefficients and the lake parameters, the estimation of the transfer coefficients was based either on bulk parameterization (Woolway et al., 2017), or was compared to other studies where there were no direct flux measurements (Panin et al., 2006).

Fewer studies have been published on the Stanton and Dalton numbers. Al-

though the measurements in the oceans showed their obvious increase at low wind speeds, both transfer coefficients were considered as fairly constant with a value of $1.1 \cdot 10^{-3}$ (review of these measurements in (Kantha & Clayson, 2000)). First measurements conducted in lakes revealed this value being higher and equal to ~$1.5 \cdot 10^{-3}$ (Harbeck, 1962; Hicks, 1972) or $1.9 \cdot 10^{-3}$ (Strub & Powell, 1987). Harbeck (1962) and Brutsaert & Yeh (1970) reported a dependence of the Dalton number on the lake surface area. Heikinheimo et al. (1999) summarized that the Dalton number is generally known to be less dependent on the wind speed. From the most recent studies (Xiao et al., 2013; Li et al., 2016; Wei et al., 2016; Dias & Vissotto, 2017), there is evidence that both coefficients depend on the wind speed and that the Stanton number is higher than the Dalton number by approximately a factor of 1.3. This indicates that the earlier assumption of the equality of both coefficients may not be valid for lakes.

The eddy-covariance (EC) technique is a micrometeorological method to directly measure momentum, heat, water vapor and greenhouse gas fluxes (Foken, 2008). It is based on the correlation between turbulent fluctuations of vertical wind speed and scalar air properties. Using this technique, one can obtain the spatial and temporal average of turbulent fluxes originating from an area called footprint and a period of meteorological stationarity (Lenschow et al., 1994; Sun et al., 2006; Burba & Anderson, 2010; Foken et al., 2012). Nowadays, the EC technique is commonly used over lakes (Blanken et al., 2000; Vesala et al., 2006; Nordbo et al., 2011; Lee et al., 2014; Mammarella et al., 2015; Spank et al., 2020; Golub et al., 2021). However, several studies reported difficulties in measuring the wind stress at weak winds, which resulted in large uncertainties (Kantha & Clayson, 2000). Low wind speed conditions are more relevant for lakes and specifically small lakes that are the most abundant inland water bodies (Downing et al., 2006).

In this study, we evaluate the first multiple water body estimates of bulk transfer coefficients and their dependencies on wind speed and water body characteristics using EC data measured above lakes. The analysis aimed at answering the following research questions: 1) what are the typical values for the bulk transfer coefficients and their variability among lakes and reservoirs? 2) how do the values compare with the reported transfer coefficients for oceans and other lakes? 3) can the mechanistic approaches mentioned above describe the transfer coefficients at low wind speed regime? 4) is there a consistent dependence of the transfer coefficients on lake characteristics, such as water depth, lake area and wind fetch? In the sections below, we examine possible answers.

2 Materials and Methods

2.1. Eddy-covariance dataset

For this analysis, most of the existing EC data measured by various researchers over lakes and reservoirs were extracted from open access databases and repositories of published papers. The fluxes that are reported in the datasets were calculated using different software (e.g., EddyPro (LI-COR, Inc, 2021), TK3

(Mauder & Foken, 2015), EddyUH (Mammarella et al., 2016)). In total, we obtained data for 23 lakes and 8 reservoirs located in the arctic, subarctic, temperate and subtropical zones (Figure 1, Table S1). The water bodies are located in different landscapes, including mountains (e.g., Lake Lunz, Austria or Lake Klöntal, Switzerland), forests (e.g., Lake Vanajavesi, Finland), and arctic landscapes. The EC mast at each lake or reservoir was installed either on a floating or bottom-fixed platform, on shore, or on small islands. The measurement height ranged between 1.3 m and 16.1 m with 2 m being the most frequent height among all datasets. Elongated shapes of the lakes or shore/island locations were the subject of wind direction filtering to ensure that the measured surface fluxes were originating from water. Approximately half of the water bodies in this study had a surface area (A_s [km^2]) smaller than 10 km^2 with an average wind fetch (F_{ave} [m]) ranging from 168 m to 1553 m. The fetch grid was estimated from the map as the distance from the measurement location to the shore with the corresponding wind direction. Then, the time series of the fetch was interpolated from this grid using the measured wind directions. The average fetch was calculated as the mean distance for the filtered wind directions. The rest of the lakes and reservoirs were larger: the maximum surface area of $2.6 \cdot 10^4$ km^2 and the maximum mean fetch of $2.6 \cdot 10^4$ m refer to one of the Great Lakes – Lake Erie in the USA. The maximum depth (D_{max} [m]) varied between 1.3 m (Lake Villasjön, Sweden) and 89 m (Rappbode Reservoir, Germany). Each EC dataset contained the estimated variables averaged over 30 min intervals.

The variables included wind speed (U_z [m s^{-1}]), wind direction (WD [°]), friction velocity (u_* [m s^{-1}]) as a quantity characterizing the momentum flux ($\tau = \rho_a u_*^2$ [kg m^{-1} s^{-2}], ρ_a – air density [kg m^{-3}]), air temperature (T_a [°C]), turbulent fluxes of sensible heat (H [W m^{-2}]), and latent heat (L_vE [W m^{-2}]), the latter referred to in this paper as water vapor flux as well. Water temperature was provided either as skin surface temperature (T_s [°C]) or bulk water temperature, measured at 0-0.5 m water depth (T_w [°C]). The skin temperature was observed with an infrared thermometer or calculated from outgoing longwave radiation, both corrected for the reflectance of incoming longwave radiation. Some lakes or reservoirs had only momentum flux data, resulting in fewer estimates of heat and water vapor transfer coefficients. Parameters such as precipitation considered as a factor for filtering the data was not available for all datasets. The duration of the EC measurements ranged from 11 days (Lake Wohlen, Switzerland) to 2243 days (or ~ 6.1 years, Lake Dagow, Germany) with a median duration of 155 days.

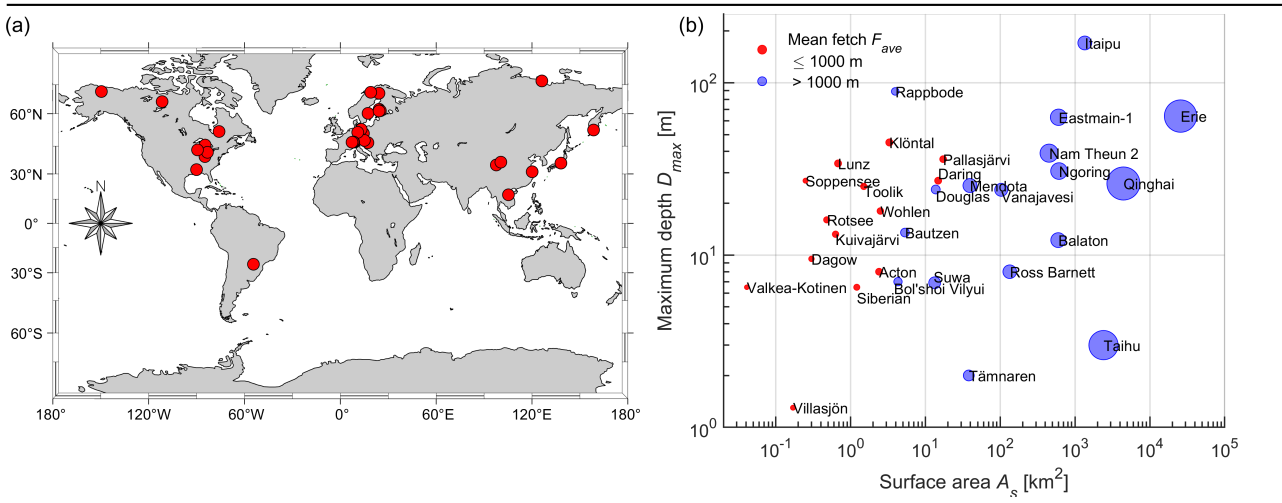

Figure 1. (a) Geographical distribution of the eddy-covariance measurements over the lakes and reservoirs u

2.2. Data filtering and averaging

The individual datasets used in the analysis were subject to filtering with the following different criteria:

1. filtering based on stationarity and integral turbulence test quality flags;
2. restriction of the wind directions to ensure >90% of footprint was originated from water;
3. removing periods with ice cover;
4. removing periods with precipitation (if data on precipitation was available);
5. removing periods with low fluxes $u_* < 0.05$ m s^{-1}, $|H|$, $|E| < 10$ W m^{-2} following, e.g., Li et al. (2016) and Wei et al. (2016);
6. removing periods with floating vegetation on the water surface (only for Lake Suwa, Japan).

Quality screening of EC data is known to be site- and instrument- specific (Burba & Anderson, 2010). The data were either available in filtered form, or they contained the quality flags provided by the software. Non-filtered datasets included quality flags for each flux value (momentum, sensible and latent heat fluxes) to ensure the stationarity of the time series (homogeneity of the flow) and developed turbulent conditions (Foken et al., 2004; Foken & Wichura, 1996).

Removing wind directions was site-specific and we carefully studied each individual site. We only accepted the data from periods when wind was blowing from

the lake with sufficient fetch. We specified the accepted wind directions for each site in Table S1. We focused on open-water conditions and discarded ice-covered periods either using the water temperature time series or interval camera data. For Lake Suwa we removed the approximate periods when floating vegetation appeared on the water surface using interval camera data, however, for other sites this kind of data was not available. For some sites, all erroneous data due to rain interference and site maintenance were filtered by data providers, or we removed periods with precipitation (if data were available). There is no common convention for selecting the thresholds of flux values for filtering the fluxes and they were taken from the literature (Wei et al., 2016). We describe the effect of these filters on the data as well as we compare different types of averaging applied to data in Text S1. This pre-analysis revealed that the logarithmic bin averaging for the derived quantities is an adequate measure to use in the following sections.

2.3. Transfer coefficients

Turbulent fluxes of momentum ( ), sensible heat (H) and latent heat (E) at the water surface are expressed as:

$$\tau = -\overline{u'w'}\rho_a = \rho_a u_*^2 = \rho_a C_D U_{10}^2, \tag{1a}$$

$$H = \rho_a c_p \overline{w'T'} = -\rho_a c_p T_* u_* = \rho_a c_p C_H U_{10} \left(T_s - T_{10}\right), \tag{1b}$$

$$L_v E = \rho_a L_v \overline{w'q'} = -\rho_a L_v q_* u_* = \rho_a L_v C_E U_{10} \left(q_s - q_{10}\right), \tag{1c}$$

where $\overline{u'w'}$ is the covariance of horizontal (u') and vertical (w') wind velocity fluctuations; $\overline{w'T'}$ [m s^{-1} K], $\overline{w'q'}$ [m s^{-1} kg kg^{-1}] are the covariances of vertical wind velocity and air temperature (T') and specific humidity (q') fluctuations. U_{10} is wind speed at 10 m height, T_s and T_{10} [K] are the surface water temperature and the air temperature at 10 m height, respectively, q_s and q_{10} [kg kg^{-1}] are the specific humidity at the air-water interface (estimated from surface temperature) and at 10 m height, respectively. c_p [J kg^{-1} K^{-1}] is the specific heat of air at constant pressure, and L_v [J kg^{-1}] is the latent heat of vaporization. $T_* = \frac{-\overline{w'T'}}{u_*}$ and $q_* = \frac{-\overline{w'q'}}{u_*}$ are temperature and specific humidity scales, respectively. The standard sign convention is that the momentum flux is defined as positive downward, while sensible and latent heat fluxes as positive upward (Kaimal & Finnigan, 1994). Using measured flux data from the obtained EC datasets, the transfer coefficients can be derived from Eq. (1a-c) as follows:

$$C_D = \frac{u_*^2}{U_{10}^2}, \tag{2a}$$

$$C_H = \frac{\overline{w'T'}}{U_{10}(T_s - T_{10})}, \tag{2b}$$

$$C_E = \frac{\overline{w'q'}}{U_{10}(q_s - q_{10})}. \tag{2c}$$

Wind speed, air temperature (T_z) and specific humidity (q_z) measured at a certain height z were converted to a standard height of 10 m considering stability of the atmosphere following the equations:

$$U_{10} = U_z - \frac{u_*}{\kappa}\left[\ln\left(\frac{z}{10}\right) - \psi_u\left(\frac{z}{L}\right) + \psi_u\left(\frac{10}{L}\right)\right], \quad (3a)$$

$$T_{10} = T_z - \frac{T_*}{\kappa}\left[\ln\left(\frac{z}{10}\right) - \psi_T\left(\frac{z}{L}\right) + \psi_T\left(\frac{10}{L}\right)\right], \quad (3b)$$

$$q_{10} = q_z - \frac{q_*}{\kappa}\left[\ln\left(\frac{z}{10}\right) - \psi_T\left(\frac{z}{L}\right) + \psi_T\left(\frac{10}{L}\right)\right], \quad (3c)$$

where κ is the von Kármán constant, L [m] is the Obukhov length, $\psi_u\left(\frac{z}{L}\right)$ is the stability function which is the integral of the empirical universal function for the momentum flux and $\psi_T\left(\frac{z}{L}\right)$ – the same for sensible and latent heat (Businger et al., 1971). In the literature, z/L is usually denoted as the non-dimensional stability parameter ζ. To remove the effect of atmospheric stability on the magnitude of the transfer coefficients, C_D, C_H, C_E are converted to their neutral counterparts $C_{\mathrm{DN}}, C_{\mathrm{HN}}, C_{\mathrm{EN}}$ (i.e. for neutrally-stratified atmospheric conditions) (Large & Pond, 1981):

$$C_{\mathrm{DN}} = \kappa^2\left[\ln\left(\frac{10}{z_0}\right)\right]^{-2} = C_D\left[1 + \kappa^{-1}\, C_D^{\frac{1}{2}}\psi_u\left(\frac{10}{L}\right)\right]^{-2}, \quad (4a)$$

$$C_{\mathrm{HN}} = C_D\left[1 + \kappa^{-1}\, C_D^{\frac{1}{2}}\psi_u\left(\frac{10}{L}\right)\right]^{-1}\left[\frac{C_D}{C_H} + \kappa^{-1}\, C_D^{\frac{1}{2}}\psi_T\left(\frac{10}{L}\right)\right]^{-1}, \quad (4b)$$

$$C_{\mathrm{EN}} = C_D\left[1 + \kappa^{-1}\, C_D^{\frac{1}{2}}\psi_u\left(\frac{10}{L}\right)\right]^{-1}\left[\frac{C_D}{C_E} + \kappa^{-1}\, C_D^{\frac{1}{2}}\psi_T\left(\frac{10}{L}\right)\right]^{-1}, \quad (4c)$$

where $z_0$is the surface roughness length. For our calculations, we used the Kansas-type stability functions (Businger et al., 1971) in the form of Högström (1988), which is the most frequently applied form (Foken, 2008). $C_{\mathrm{DN}}, C_{\mathrm{HN}}, C_{\mathrm{EN}}$ were estimated for 31, 24, 23 water bodies under study, respectively, depending on the flux data availability (see details about each lake or reservoir in Table S1 and in data repository 10.5281/zenodo.6597829). After calculation of C_H, C_E (Eq. 2b-2c), we removed negative values that were a result of the inconsistency between sign of the measured flux and the temperature difference (probably related to the measurements random uncertainty).

In the scientific community, there has been an ongoing discussion on the form of the transfer coefficients to be presented. For example, some studies focused only on neutral values of the drag coefficient (Li et al., 2016) or some considered the drag coefficient non-adjusted to their neutral counterpart (C_D). Other studies addressed the so-called "effective" drag coefficient, which was derived as the slope coefficient for the linear relationship between u_*^2 and U_{10}^2 (Xiao et al., 2013). We examine the difference between C_D, C_H, C_E and $C_{\mathrm{DN}}, C_{\mathrm{HN}}, C_{\mathrm{EN}}$ in Section 3.1.

2.4. Parametrizations of the drag coefficient at low and high wind speeds

2.4.1. *Smooth flow*

Previous studies focused on the parameterizations of surface roughness length z_0 (see Eq. 4a) to assess wind speed dependence of the drag coefficient (e.g., Ataktürk & Katsaros (1999). In our study, we compared C_{DN} estimated from measured momentum fluxes with the existing approaches. One of the approaches is based on the smooth flow regime at low wind speed (< 3 m s^{-1}), where the thickness of the viscous sublayer (δ_ν) determines the aerodynamic roughness of the interface (Schlichting, 1968), and not the physical roughness of the water surface:

$$\delta_\nu = z_0 = \alpha \frac{\nu}{u_*}, \quad (5)$$

where $\alpha = 0.11$ and $\nu = 1.6\ \times 10^{-5}$ [m^2 s^{-1}] is kinematic viscosity of air. z_0 can be derived from Eq. 4a as:

$$z_0 = z\ \exp\left(-\frac{\kappa}{\sqrt{C_{\mathrm{DN}}}}\right). \quad (6)$$

Substituting Eq. 6 into Eq. 5, replacing $u_* = \sqrt{C_{\mathrm{DN}}} U_{10}$ and taking the standard height as $z = 10$ m, we obtain the following expression for smooth flow approach:

$$\frac{1}{\sqrt{C_{DN\_SF}}} = \frac{1}{\kappa} \ln\left(\frac{z\sqrt{C_{DN\_SF}} U_{10}}{\nu}\right) - \frac{1}{\kappa} \ln(\alpha), \quad (7)$$

We used measured values of U_{10} as input and solved Eq. 7 iteratively for C_{DN_SF}.

2.4.2. *Capillary waves*

As an alternative method to estimate C_{DN} at low wind speeds, we considered the approach proposed by Wu (1994). He suggested that the wind shear stress in the absence of large gravity waves is related to the ripples (capillary waves). For the capillary waves, the roughness length is related to surface tension ( ) as:

$$z_0 = \alpha_{\mathrm{Wu}} \frac{\sigma}{\rho_w u_*^2}, \quad (8)$$

where $_{Wu} = 0.18$ is an empirical constant and ρ_w is water density. Surface tension at a temperature of 20°C is $= 7.28{\cdot}10^{-2}$ N m^{-1}. In analogy to the smooth flow approach, substitution of Eq. 6 to Eq. 8 and replacement of u_* leads to the expression:

$$\frac{1}{\sqrt{C_{DN\_CW}}} = \frac{1}{\kappa} \ln\left(\frac{z\rho_w C_{DN\_CW} U_{10}^2}{\mathrm{w}}\right), \quad (9)$$

Eq. 9 was solved iteratively for C_{DN_CW} using wind speeds U_{10} from the data sets and z = 10 m.

2.4.3. *Charnock relationship*

With increasing wind speed, the thickness of the viscous sublayer becomes smaller, and the aerodynamic roughness of the water surface (z_0) becomes minimal, before surface gravity waves evolve. At wind speeds exceeding 3 m s^{-1}, waves protrude from the viscous sublayer and surface roughness length increases with increasing wind speed, indicating the transition from a smooth to a rough flow regime. Charnock, (1955) proposed the following equation for surface roughness length over fully developed surface waves, which account for typical oceanic conditions:

$$z_0 = \beta \frac{u_*^2}{g}, \quad (10)$$

where ranges from 0.011 to 0.0185 (Garratt, 1994), g is the gravitational acceleration. Substitution of Eq. 6 into Eq. 10 leads to the following implicit equations that was iteratively solved for C_{DN_CH}.

$$\frac{1}{\sqrt{C_{DN\_CH}}} = \frac{1}{\kappa} \ln\left(\frac{\mathrm{gz}}{C_{DN\_CH} U_{10}^2}\right) - \frac{1}{\kappa} \ln(\beta). \quad (11)$$

2.4.4. *The concept of gustiness*

Grachev et al., (1998) suggested that under strong convective conditions, the wind stress at the water surface is predominantly governed by random convective motions - gusts - in the convective boundary layer (CBL), whereas the mean wind speed vector can even become zero (Godfrey & Beljaars, 1991). These large convective eddies embrace the entire CBL and affect the turbulence regime in the atmospheric surface layer. Grachev et al. (1998) formulated a new approach to estimate the drag coefficient using this concept. According to their study, the gustiness could explain the apparent increase of the drag coefficient estimated using the traditional equation (Eq. 2a, 4a) at low wind speeds. The estimated drag coefficient accounting for gusts was a factor of 1.5 to 6 smaller at wind speeds below 2 m s^{-1} in comparison with the drag coefficient calculated from Eq. 2a, 4a. The gustiness concept is widely accepted and used in the COARE algorithm to estimate air-sea fluxes (Fairall et al., 2003).

The effect of gustiness on the drag coefficient can be accounted for by the so-called gustiness factor G, which corresponds to the ratio of the scalar-averaged

($\widetilde{U}_{10}$) to vector-averaged wind speed. Following (Grachev et al., 1998), G can be parameterization in terms of the convective velocity scale w_*:

$$G^2 = \frac{\widetilde{U}_{10}^2}{U_{10}^2} = 1 + \left(\frac{\gamma w_*}{U_{10}}\right)^2, \quad (12)$$

where $\gamma = 1.2$ is an empirical constant (Beljaars, 1995) and w_* is expressed as:

$$w_* = \left(g z_i \frac{\overline{w'T_v'}}{T_v}\right)^{1/3}, \quad (13)$$

where, T_v [K] is the virtual temperature, z_i is the CBL height, defined as the height of the lowest inversion. Previous studies used the fixed height of the CBL equal to 1000 m (Beljaars, 1995). We denote two corresponding types of gustiness factor as G_{wind} and G_{conv}.The new relationship between neutral gustiness drag coefficient C_{DNG} and its gustiness counterpart $\widetilde{C}_{\text{DG}}$ is:

$$C_{\text{DNG}}^{-1/2} = \widetilde{C}_{\text{DG}}^{-1/2} + \frac{\psi_u(\frac{z}{L})}{\kappa}, \quad (14)$$

where $\widetilde{C}_{\text{DG}} = C_{\text{DG}}/G^2$ and $C_{\text{DG}} = \left(\frac{\widetilde{u}_*}{U_{10}}\right)^2$, where $\widetilde{u}_*$ is the scalar-averaged friction velocity. Akylas et al. (2003) investigated the combinations with different averaging procedures and suggested that vector-averaged friction velocity u_* is more appropriate to use with scalar-averaged wind speed for all wind speed classes. We applied this approach for cases with unstable atmosphere ($\zeta < 0$) using the stability functions described in Grachev et al. (1998).

3 Results

3.1. Transfer coefficients over lakes

Bulk transfer coefficients for neutral atmospheric stability C_{DN}, C_{HN} and C_{EN} (Eq. 4a-4c) were estimated using data from 23 lakes and 8 reservoirs (see data availability details in Table in the data repository 10.5281/zenodo.6597829). The transfer coefficients varied between the water bodies and differed on average by a factor of 2-3 for wind speeds exceeding 3 m s^{-1}. However, we identified three water bodies for which the estimated drag coefficients (C_{DN}) were exceptionally large at all wind speeds (up to a factor of five, Lake Quinghai, China, Nam Theun 2 Reservoir, Laos), or exceptionally low (factor of four, Bol'shoi Vilyui Lake, Russia), when compared to other water bodies with similar surface area. These three water bodies contributed largely to the variability among systems (Figure S4a shows the result without these three sites, Figure S5a shows the estimates for individual water bodies). Similarly, Dalton numbers (C_{EN}) estimated

from data measured at Lake Lunz (Austria) were a factor of three higher than for other water bodies (Figure S5c). Stanton numbers (C_{HN}) calculated from the dataset collected at Itaipu Reservoir (Brazil) were a factor of four lower than other estimates. Most (90%) of the C_{HN} estimates were removed by filtering for low flux values at this reservoir. With only one of the peculiar data sets for each of the two transfer coefficients, they did not affect the overall statistics for C_{HN} and C_{EN}. We did not find possible sources of errors and considered these data as outliers. In the overall estimates and in the range of variability shown in Figure 2a, we included the complete dataset.

All transfer coefficients showed a similar wind speed dependence (Figure 2a,b,c). At high wind speeds (> 3 m s^{-1}), C_{DN}, C_{HN}, C_{EN} had relatively constant values of $2 \cdot 10^{-3}$, $1.5 \cdot 10^{-3}$, $1.1 \cdot 10^{-3}$, respectively. All transfer coefficients increased towards the lowest wind speeds. The strongest increase was found for C_{DN}, which was one order of magnitude higher ($2.3 \cdot 10^{-2}$) at the lowest wind speed (0.5 m s^{-1}, the first bin) compared to values at higher wind speeds. A similar, but less pronounced increase was observed for C_{HN} and C_{EN}: their values at the lowest wind speed were $6.5 \cdot 10^{-3}$ and $3.2 \cdot 10^{-3}$, respectively. The mean ratio of C_{HN} to C_{EN} is 1.4 and has its maximum value at low wind speeds and a minimum of 1.2 at wind speeds of 3.5-6.5 m s^{-1} (Figure 3).

Unstable atmospheric conditions ($\zeta < 0$) prevailed over all water bodies, particular during the evening and at night time, when $> 80\%$ of all data were obtained under unstable conditions (Figure 2d). Stable atmospheric conditions occurred most frequent during the day (12-19 hours). In addition, we estimated the percentage of time when the wind speed was less than 3 m s^{-1} (Figure 2e). Low wind speed conditions prevailed slightly during the evening and at night, when the atmosphere was mostly unstable. This means that the significant increase of the transfer coefficients at low wind speeds frequently coincides with unstable atmospheric conditions, when the water is still warm and the atmosphere starts cooling at the end of the day.

To analyze the effect of atmospheric stability on the transfer coefficients, we compared the transfer coefficients (C_D, C_H, C_E, Eq. 2a-2c) with their neutral counterparts (C_{DN}, C_{HN}, C_{EN}, Eq. 4a-4c, Figure S6). We found that atmospheric stability did not significantly affect the values of C_D, C_H and C_E at wind speeds exceeding 3 m s^{-1}: their values were in close agreement with C_{DN}, C_{HN} and C_{EN}. However, it is evident that at low wind speeds (0-2 m s^{-1}) these transfer coefficients under in-situ conditions were systematically higher (up to a factor of 2-3) than their neutral counterparts C_{DN}, C_{HN} and C_{EN}.

Estimation of C_H and C_E (Eq. 2b, 2c and Eq. 4b,4c) involves water surface temperature, for which the skin temperature is the most appropriate measure. However, these measurements were not available for some sites. Instead, we used water temperature measured at some depth (often varying between 0 and 0.5 m between datasets). We compared three types of calculations of C_H using two subsets which use: (a) only skin temperature (b) only water temperature and (c) the total dataset which includes both types of temperature measurements

(Figure S4b). C_{HN} estimated with water temperature tends to be slightly lower than the estimates using skin temperature (the percentage difference is approximately 10%). As a result, we presented C_H and C_E (Figure 2b,c) calculated using all available data, independent of how water surface temperature was measured. When both the skin and water temperatures were available for one site, the skin temperature was used.

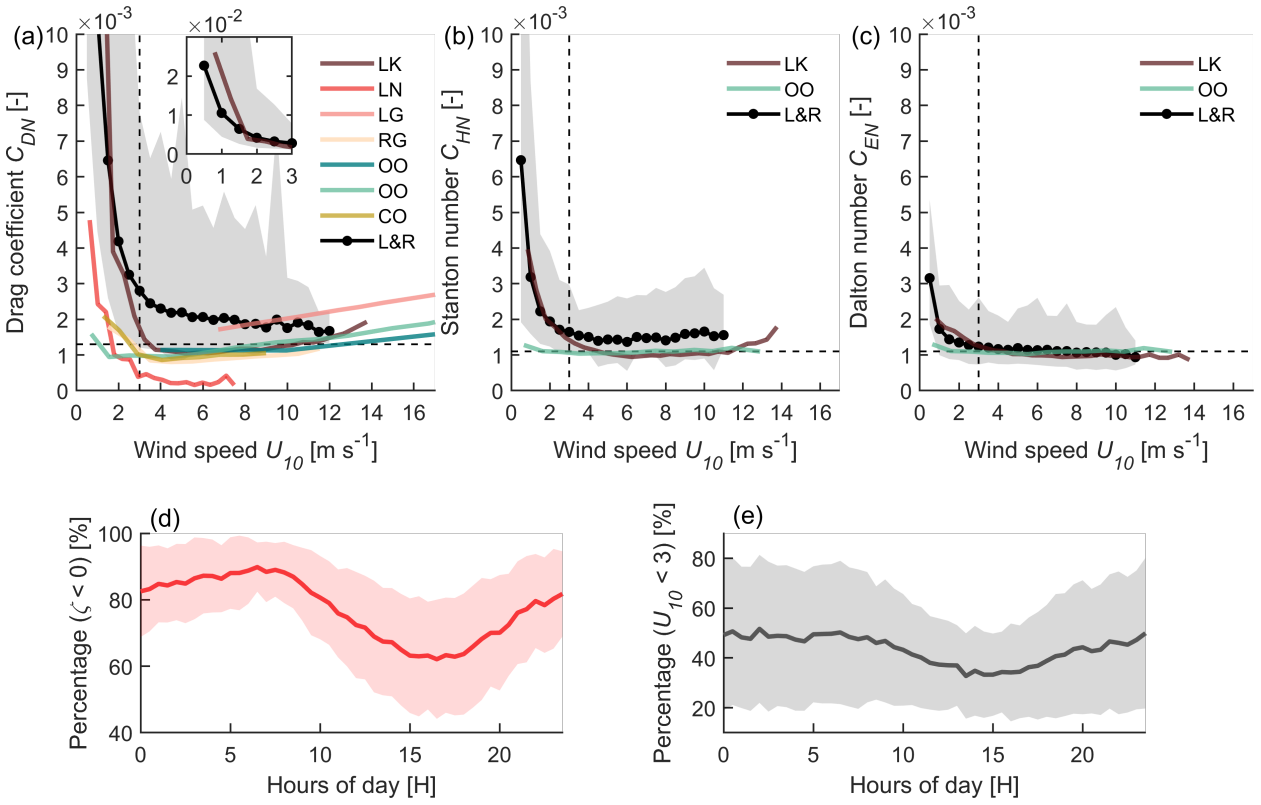

Figure 2. Neutral (a) drag coefficient (C_{DN}), (b) Stanton number (heat transfer coefficient, C_{HN}), (c) Dalton

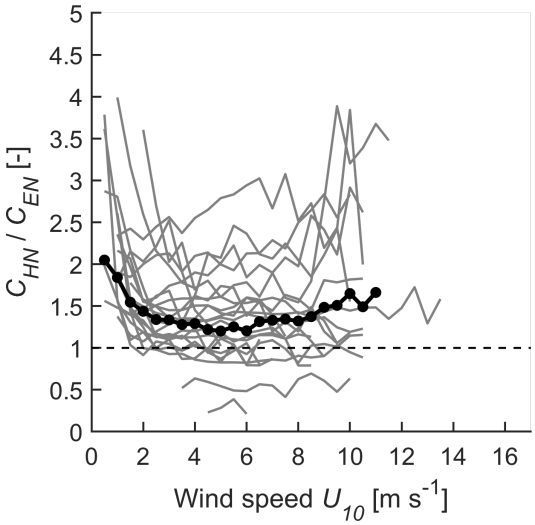

Figure 3. Ratio of bin-averaged C_{HN} to C_{EN} estimated for each individual dataset (21 water bodies, shown l

3.2. Parametrizations of the drag coefficient

We examined the possible mechanisms (Eq. 7, 9, Section 2.4) that could explain the increase of the drag coefficient at low wind speeds and we tested the Charnock relationship (Eq. 11), which describes its wind speed dependence at high wind speeds (Figure 4a). It is evident that our estimates of C_{DN} at wind speeds exceeding 3 m s^{-1} were higher (around factor of two) than the that predicted by the model proposed by Charnock, (1955).

The discrepancy between the EC-derived C_{DN} and theoretical models from the literature showed that neither the concept of smooth flow, nor the consideration of capillary wave roughness could explain the sharp increase of C_{DN} at low wind speeds (Figure 4a). We found that the function describing the wind speed dependence of the drag coefficient proposed by Liu et al. (2020) based on EC measurements over terrestrial surfaces ($C_{\mathrm{DN}} = b_1\,[1 + b_2 \exp(b_3 U_{10})]$) could successfully describe the relationship over all lakes (Figure 3a). In a similar way, we applied this empirically derived function to C_{HN} and C_{EN} estimates (Figure S7). The fitted coefficients for our data are provided in Table 1.

The concept of gustiness was proven to be relevant for the drag coefficient at low wind speeds at least in the marine environment (Section 2.4.4). We considered this alternative approach to estimate the drag coefficient using one dataset collected in Lake Suwa, Japan, for which scalar averaged wind speeds could be calculated in addition to the commonly provided vector averaged wind speeds (Figure 4b). We calculated the drag coefficient considering gustiness (C_{DNG} , Eq. 14) using the gustiness factor derived from both types of wind speeds (G_{wind}),

and from the parametrization using the convective velocity scale (G_{conv}) for unstable atmospheric conditions and used C_{DN} (Eq. 3a) for stable conditions. At wind speeds less than 3 m s^{-1} C_{DN} was on average a factor of 1.3 higher than C_{DNG} (when using G_{wind}). The ratio reached its maximum of 1.9 at the lowest wind speed (0-0.5 m s^{-1}). The ratio of C_{DN} to C_{DNG} estimated using G_{conv} was approximately a factor of 1.2 higher than the one that was estimated using G_{wind}.

Table 1. Coefficients for the empirical function $C = b_1\,[1 + b_2\exp(b_3 U_{10})]$ (Liu et al., 2020)), describing the v

C_{DN}
C_{HN}
C_{EN}

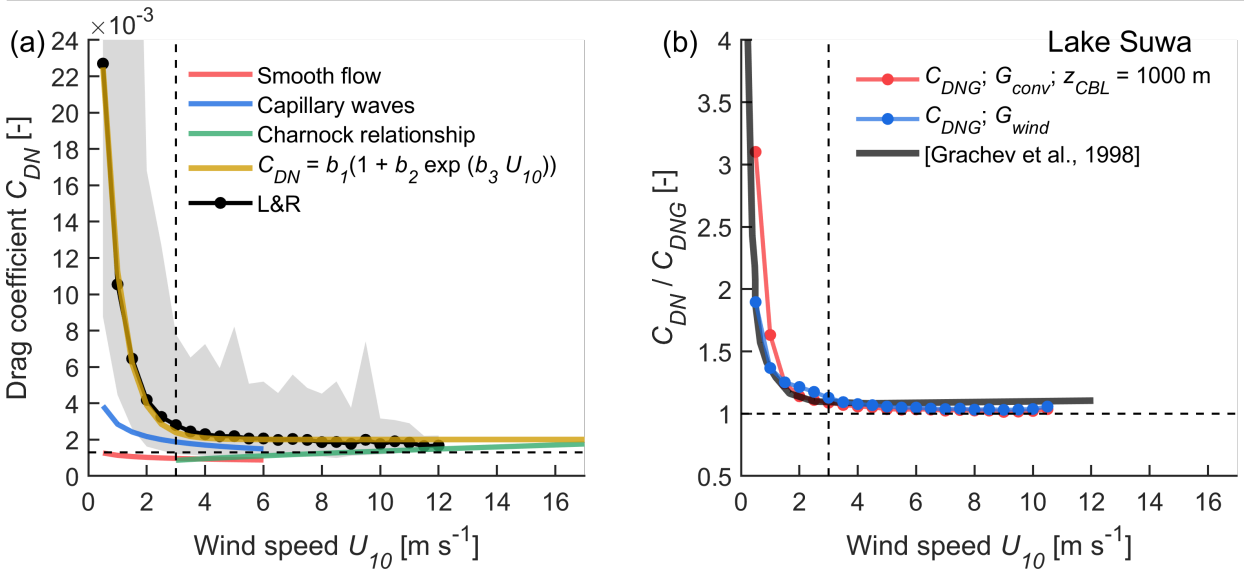

Figure 4. (a) Bin-averaged C_{DN} versus U_{10}. Black line with symbols (L&R): C_{DN} obtained from EC measur

3.3. Dependence of the bulk transfer coefficients on the lake characteristics

We examined the dependencies of the bulk transfer coefficients on lake characteristics, including the maximum and average water depth, water depth at the measurement site, maximum and average wind fetch, and water surface area. As the transfer coefficients at high wind speeds were relatively constant, we first analyzed effects of lake characteristics on the mean values of the transfer coefficients for wind speeds exceeding 3 m s^{-1} estimated for each individual water

body.

We found that the mean C_{DN} decreased significantly (Pearson correlation coefficient r = -0.5, p-value < 0.05) with increasing lake surface area and with increasing mean and maximum fetch (Figure 5a, 5b and Figure S8a). These relationships could be expressed as power law dependencies ($y = x^A \exp(\mathrm{B}\ \ln 10)$, where A and B are the slope and intercept of the linear regression $\log_{10} y = A\ \log_{10} x + B$) with exponents of -0.07 and -0.16, -0.12, respectively. Most variability in C_{DN} was found to be explained by the lake surface area (for log-transformed data the coefficient of determination was $\mathrm{R}^2 = 0.3$). The correlation between C_{DN} and mean fetch was slightly higher than for maximum fetch (-0.5 versus -0.4). A principal component analysis revealed that lake surface area has a largest predictive power (Figure S9). We did not find a significant correlation ($r \sim$ -0.2, p-value > 0.05) between the mean C_{HN}, C_{EN} and surface area, mean, and maximum fetch, the stronger correlation could be found when considering data at fixed wind speeds. Significant correlation was found between C_{EN} and the surface area at fixed wind speed of 6 m s^{-1} (Figure 5g). In addition, there was weak negative correlation with mean and maximum fetch ($r \sim$ -0.4, Figure 5h and Figure S8g).

Using the principal component analysis, we identified that there was no significant correlation of the averaged transfer coefficients at high wind speeds with maximum, average or local water depth (Figure 5c,f,i, Figure S8, S9). We used the exponential dependence from Panin et al. (2006) to compare with our results. However, we did not have sufficient sites with larger depth to confirm any dependence.

At low wind speeds (< 3 m s^{-1}), the transfer coefficients were strongly wind speed dependent (Figure 2a,b,c) and their relationships with lake characteristics are examined separately for each different wind speed interval. Here we found that C_{DN} and C_{HN} significantly increased with increasing water surface area for wind speeds between 0.5 m s^{-1} and 2 m s^{-1}. At higher wind speeds these correlations become negative, as in the analysis for wind speed > 3 m s^{-1} presented above. As an example, we show the transfer coefficients for a wind speed of 1 m s^{-1} in Figure S10. Significant correlation ($r \sim 0.5$) (and its decreasing towards high wind speeds) could also be observed between C_{DN}, C_{DN} and mean and maximum fetch (data not shown). At the same time, we found significant correlations of all three transfer coefficients with measurement height at low wind speeds, which was not present at high wind speeds (Figure S10d-f).

As a final step, we looked at the possible relationship between the averaged wind speed (estimated over entire time series for each individual water body) and surface area. We found a significant correlation between them in a double-logarithmic domain ($r = 0.5$, p-value < 0.05, Figure S11), resulting in a power-law dependence $U_{10} = A_s^{0.05} \exp(0.5\ \ln 10)$.

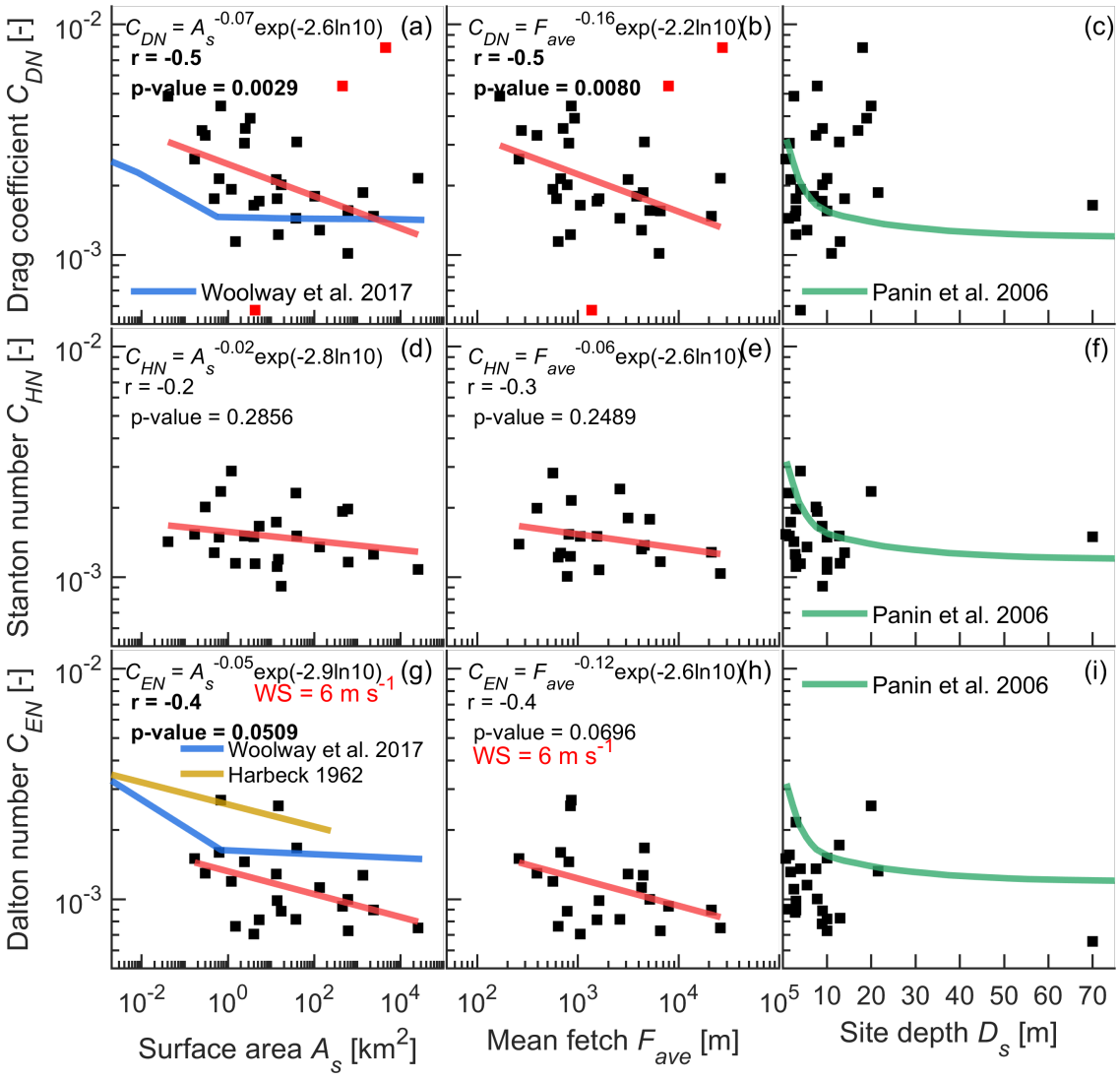

Figure 5. Neutral transfer coefficients (a, b, c) C_{DN}; (d, e, f) C_{HN}; (g, h, i) C_{EN} versus surface area of the w

4 Discussion

4.1. Bulk transfer coefficients estimated for lakes and reservoirs

We examined the bulk transfer coefficients describing the transport of momentum, heat and water vapor at the water surface estimated based on EC data collected at 23 lakes and 8 reservoirs of different size, depth, and location. All transfer coefficients tended to increase towards low wind speeds and remained

relatively constant at wind speeds exceeding 3 m s^{-1}. This increase was reported in previous studies for lakes (see, e.g., Wei et al., 2016; Xiao et al., 2013) and has been extensively investigated but has remained unexplained up to now. The lower bound for C_{DN}, C_{HN}, C_{EN} among the water bodies at high wind speeds were within the range reported by previous studies – either for large lakes (> 200 km^2, (Kuznetsova et al., 2016; Wei et al., 2016)) or for the marine environment: classical open ocean measurements (Fairall et al., 2003; Large & Pond, 1981) and coastal ocean sites under fetch-limited conditions (Lin et al., 2002). Indeed, we also considered large lakes (Figure 1b) that were expected to have the smallest drag coefficient as they had the largest fetch (e.g., Lake Erie, Lake Taihu, Lake Balaton). The mean C_{DN} for winds exceeding 3 m s^{-1} was equal to $2 \cdot 10^{-3}$ and this value corresponded to an upper bound for the water surface roughness (0.001 m) reported by Foken (2008), but was a factor of two higher than the values reported for oceans and large lakes or reservoirs (Large & Pond, 1981; Fairall et al., 2003). While C_{HN} and C_{EN} are commonly assumed to be equal, we found that C_{HN} was on average by a factor of 1.4 higher than C_{EN} (averaged over all wind speeds and all water bodies under study). The finding of C_{HN} being higher than C_{EN} confirmed the results reported by, e.g., (Wei et al., 2016; Dias & Vissotto, 2017). The mean value of C_{EN} for high wind speeds ($1.1 \cdot 10^{-3}$) was found to be the same as in (Kantha & Clayson, 2000), but C_{HN} was larger ($1.5 \cdot 10^{-3}$) as in (Harbeck, 1962; Hicks, 1972). The fact that $C_{HN} > C_{EN}$ may have significant implications, because it results in biased estimates of lake evaporation based on the energy-budget Bowen ratio method.

Values of C_{DN} varied considerably depending on the type of measurements used for its estimation. For example, in (Simon, 1997) C_{DN} was calculated from the dissipation rate measured at the water side for relatively large Lake Neuchâtel (218 km^2, Switzerland). C_{DN} was significantly lower than our estimates (factor of ten) and the estimates from lakes or marine measurements (factor of five). However, these estimates also confirmed the increase of C_{DN} at low wind speeds. C_{DN} at high wind speeds calculated from the wind profile method at the nearshore site in Lake Geneva (Graf et al., 1984) was in close agreement with our estimates. The strong increase of C_{DN}, C_{HN}, C_{EN} at low wind speeds was similar to the one observed for a large lake with the same EC method of estimation the surface fluxes (Wei et al., 2016), but it was not supported by measurements in the marine environment.

4.2. Bulk transfer coefficients at high winds

The estimated C_{DN} at high wind speeds was higher than predicted by Charnock relationship. This result was expected as Charnock relationship is based on the assumption that the water surface roughness is controlled by fully developed surface gravity waves. This may not be the case for many lakes, where wave generation is fetch-limited (e.g., overview in (Ataktürk & Katsaros, 1999)). We could attribute this difference to the lake surface area and the average and maximum wind fetch at the measurement location. To support this, we found that the C_{DN}, C_{HN} and C_{EN} were highest in small water bodies and decreased with

increasing surface area and fetch lengths for wind speeds exceeding 3 m s^{-1}. As approximately half of the water bodies under study are relatively small (surface area < 10 km^2), our data indicated that they contributed disproportional to the higher transfer coefficients. For large lakes, the transfer coefficients at high wind speed tended to be lower and closer to the values reported in previous studies and predicted by Charnock relationship. At these higher wind speed, the surface gravity waves could potentially reach the fully developed state in large water bodies. We found a significant correlation between C_{DN}, C_{EN} and the lake surface area. The resulting C_{EN} dependence on surface area with the power of -0.05 confirmed the findings of previous studies (Harbeck, 1962; Brutsaert & Yeh, 1970). However, the values of C_{EN} in our analysis were approximately a factor of two lower. Our results could not confirm a bilinear decrease of C_{DN} with increasing lake size with a weaker dependence for large lakes, as estimated by Woolway et al. (2017) (Figure 6a). The difference between the relationship of C_{DN} with lake surface area reported in Woolway et al. (2017) could be attributed to fact, that they estimated the transfer coefficients from measurements of mean wind speed by applying the parameterizations of surface roughness for smooth flow (Eq. 5) and Charnock relationship (Eq. 10). Nevertheless, the power dependence for lakes with surface area < 1 km^2 (Woolway et al., 2017) looked similar to the one we observed (power of -0.07) for all lakes and reservoirs, suggesting that it could be generalized to many water bodies. In contrast to the results reported in (Panin et al., 2006), we did not find evidence for the existence of an influence of water depth on the bulk transfer coefficients.

4.3. Bulk transfer coefficients at low winds

Low wind speeds are typical conditions for lakes (Woolway et al., 2018), especially for smaller ones (Figure S10), which are most abundant by number (Downing et al., 2006). The most pronounced increase in bulk transfer coefficients at low wind speed was observed for C_{DN}, which was up to one order of magnitude higher at low wind speeds compared to its value at high wind speeds. We found less pronounced increases of C_{EN} and C_{EN} but their values at low wind speed can be larger up to factor of six and three, respectively, in comparison to their constant values at high winds. Periods with low wind speeds mostly corresponded to periods with unstable atmospheric conditions or enhanced convective transport, which is the most prevailing condition for all studied lakes during the ice-free period (Read et al., 2012; Woolway et al., 2017).

None of the tested approaches, including smooth flow and capillary wave parametrizations, could explain the strong increase for C_{DN} at low wind speeds. While Wei et al., (2016) suggested that the contribution of gusts (different formulation of the C_{DN}) was not significant in their dataset, we found that the increase is partially attributed to the way of the calculation of C_{DN}. Different formulation involving the gustiness factor (G_{wind}) could reduce the values of C_{DN} up to a factor of two at wind speeds of 0.5 m s^{-1}. The two different estimates of the gustiness factor (G_{wind} and G_{conv}) should have given similar results, if the correct height of the convective boundary

layer was used. However, our estimates of C_{DNG} using G_{conv} were higher than C_{DNG} using G_{wind}, which we consider as a reference. This may indicate that a fixed CBL height of 1000 m was incorrect and should have smaller values. According to Oke (1987) and Stull (1988) the CBL starts to grow during the daytime, when the ground warms the atmosphere. The observed increase of C_{DN} corresponded to the data during evening and night hours, when unstable atmospheric conditions in the surface layer above water were dominant (Figure 3d, e). While the land starts cooling and the atmosphere becomes stable in regular daily cycle, the thermal internal boundary layer (TIBL), several tens of meters thick (Glazunov & Stepanenko, 2015), may grow above the lakes at this time. The TIBL develops due to the temperature difference between land and water. Above this layer (as well as stable layer above the land), there still could be the residual layer which is left from the CBL during the day. Thus, large convective eddies may entrain this air from the residual layer. Tests with the CBL height of 10 m (not shown) led to much lower values of C_{DNG} (approximately a factor of two) compared to the reference. It remains unclear which CBL height should be used for a correct parameterization of C_{DNG}, if the scalar-averaged wind speed is not available.

The wind speed dependence of the bulk transfer coefficients (especially at low winds), could be well described by an empirical function that was originally proposed for the land surface (Liu et al., 2020). This suggests that similar physical processes control the increase in transfer coefficients at low winds, which are independent of the specific roughness conditions of water surfaces. We suggest that the reason for this increase to some extent was a contribution of large convective eddies or non-local effects as described in Liu et al. (2020) and other closely related studies (Read et al., 2012; Sahlée et al., 2014; Ala-Könni et al., 2021).

Unexpectedly, we found that the transfer coefficients (C_{DN} and C_{HN}) significantly increase with increasing lake surface area, mean and maximum wind fetch for wind speeds less than 2 m s^{-1}. This result is counterintuitive, because at low winds we did not expect a dependence on lake surface area or fetch, as it should only be important for the development of surface waves, which appears to be only around the wind speed of 3 m s^{-1} (Simon, 1997; Guseva et al., 2021). It may be related to the development of the TIBL above lakes but the potential mechanism remains unknown. At the same time, we found the significant positive correlation between the transfer coefficients and the measurement height, which was also unexpected. This finding could be a result of the measurement limitations and it could potentially attribute to the increase of the bulk transfer coefficients at low wind speeds. These issues require a separate detailed investigation.

4.4. Study limitations

The estimated bulk transfer coefficients show large scatter, even after filtering the data. The scatter is particularly high at light winds, i.e., in the first three to four wind speed intervals used for bin-averaging (0.5 – 2 m s^{-1}). It could

be associated with limitations of the EC measurements, namely, the validity of the underlying assumptions, including the homogeneity and stationarity of the flow, as well as by increasing random errors. As there are no common thresholds, for example, for the removal of low flux values, and the quality check of the EC results is very specific to each site, these effects may not have been removed completely by data filtering. In our case, applying the filter with low fluxes led to increase in transfer coefficients at low wind speeds (0-0.5 m s^{-1}) up to a factor of 1.6 which was a largest impact on the data among other filters (Text S1). However, the most recent study (Ala-Könni et al., 2021) argue that these thresholds for fluxes are not very important for the data quality filtering. Moreover, our estimates of C_{DN} differ from former results obtained using different types of measurements, such as water-side energy dissipation rates (Figure 3a, e.g., (Simon, 1997)). Thus, the combination of water- and air side measurements could be beneficial for further investigation of the bulk transfer coefficients.

Hwang (2004) suggested that the standard height of 10 m at which the transfer coefficients are reported is inappropriate for analyzing C_{DN} and its dependence on surface roughness under wave conditions. They argue that the only relevant parameter that could serve as a reference height is the wavelength that describes the decay rate of the waves with the distance from the water surface. The adjustment of the transfer coefficients to 10 m height may not be very relevant for lakes and reservoirs and the flux measurements at two different heights should be considered in future measurements. These measurements would additionally provide confirmation for the existence of a constant flux layer, which is another important assumption underlying EC measurements.

4.5. Broader implications

Bulk transfer coefficients are usually applied in numerical models for the atmospheric boundary layer, as well as in hydrodynamic models of lakes and reservoirs. Currently, the global modeling studies focusing on the lake mixing and phytoplankton blooms for climate change predictions use constant coefficients, including C_{DN} (Jöhnk et al., 2008; Read et al., 2014; Woolway & Merchant, 2019; Grant et al., 2021), or consider C_{DN} as a tuning parameter of the models (Stepanenko et al., 2014). Inadequate values of C_{DN} result in biased estimates of the current velocities in lake models (Chen et al., 2020). The increase of the transfer coefficients at low wind speeds observed in our analysis can therefore lead to significant errors, as these conditions are the most prevailing conditions for lakes. The empirical parameterizations of the wind-speed dependence of bulk transfer coefficients provided in Table 1 can potentially be applied in modeling lake-atmosphere interactions and for more accurate estimation of the surface fluxes. The dependence on the lake surface area is more complicated to implement, as we observed contrary dependencies for low and high wind speeds.

We emphasize that the Bowen-ratio method, which is frequently used to estimate evaporation may be biased given our finding that $C_{\mathrm{HN}} > C_{\mathrm{EN}}$. This finding violates the assumption of their equality in the Bowen ratio energy budget and

related methods, and implies larger (smaller) sensible heat (latent heat) fluxes than those predicted under that assumption. Both the physical mechanisms underlying their difference and the extent of the differences in the predicted sensible and latent heat fluxes require further investigation.

In state-of-the-art weather and earth system models, lakes are included as separate tiles in the model cells, where the surface fluxes over the tiles are computed via Monin-Obukhov similarity scaling. The models provide constant meteorological variables for each grid cell, which is a so-called blending height concept (von Salzen et al., 1996). To use the bulk transfer coefficients derived in this study to compute fluxes, specific values of wind, temperature and humidity over lakes should be used, which can be obtained in generalization of the tile approach, involving the parameterization of internal boundary layers over contrasting surfaces (Arola, 1999; Molod et al., 2003; de Vrese et al., 2016). MacKay (2019) presents a specific example of such an approach developed for lakes and wind speed only. Our results demonstrate a good potential of wind-gust concept to explain the observed increase of bulk exchange coefficients under low winds. However, direct incorporation of this concept in current weather models is not feasible, as these models normally do not predict scalar-averaged wind speed. A possibility to alleviate this obstacle is to replace the scalar-averaged wind speed by another measure of wind speed variability, e.g., the square root of the horizontal turbulent kinetic energy component (Castelli et al., 2005; Esau et al., 2018), or to use a parameterization of the convective velocity scale. However, the latter requires knowledge of the convective boundary layer height above the lake, which is not well understood.

5 Conclusions

We were the first to analyze the bulk transfer coefficients of momentum, sensible and latent heat from the directly measured surface fluxes above various lakes and reservoirs. We observed a pronounced increase of the transfer coefficients at low wind speeds (< 3 m s^{-1}) and relatively constant values at high wind speeds (> 3 m s^{-1}). At high wind speed, the estimated transfer coefficients generally agreed with the results provided by previous studies for large lakes and oceans, yet the Stanton number was systematically higher than the Dalton number by a factor of 1.4, which has implications for the Bowen ratio method. At high wind speed, the drag coefficient and the Dalton number decreased with increasing surface area of the water body and with increasing fetch length, whereas the opposite was found at low wind speed. The strong increase in the transfer coefficient at low wind speed could not be explained by known mechanisms, including smooth flow and capillary waves. However, it can be partly explained by the existence of gusts under unstable atmospheric conditions, and potentially by additional non-local effects. The bulk transfer coefficients at all wind speeds were well described by an empirical function that has been proposed for the land surface. Using this function could potentially improve the accuracy of the bulk parametrization of surface fluxes in numerical models for lake hydrodynamics and atmospheric dynamics. We underline the need for simultaneous measurements of waterside

and airside turbulent fluxes in future investigations, as well as experimental confirmation of the validity of the assumptions underlying eddy-covariance flux measurements at low wind speed.

Acknowledgments

S. Guseva and A. Lorke were financially supported by the German Research Foundation (Deutsche Forschungsgemeinschaft, DFG, grant LO1150/12-1). N. Dias and F. Armani were supported by research project FUNPAR 2882, with funding provided by CHESF (São Francisco Hydroelectric Company). A.R. Desai acknowledges support from the DOE Ameriflux Network Management Project and the NSF North Temperate Lakes LTER (#DEB-2025982). Funding for the AmeriFlux data portal was provided by the U.S. Department of Energy Office of Science. H. Iwata was supported by the Japan Society for the Promotion of Science KAKENHI grant number 17H05039 and 21H02315. J. Jansen was supported by the Swedish Research Council under VR grant number 2020-06460. G. Lükő was supported by the ÚNKP-21-3 New National Excellence Program of the Ministry for Innovation and Technology, Hungary. Data processing for Bol'shoi Vilyui Lake made by I. Repina was partially supported by a grant of the Russian Science Foundation 21-17-00249. T. Sachs was funded by a Helmholtz Young Investigators Grant (VH-NG-821) and infrastructure at Lake Dagow was operated as part of the Terrestrial Environmental Observatories Network (TERENO) of the Helmholtz Association of German Research Centers. K. Scholz was supported by the Austrian Academy of Sciences (ÖAW) as part of the project "Influence of climate extremes on C cycling dynamics across the boundaries of aquatic ecosystems (EXCARB)" and by the Autonome Provinz Bozen-Südtirol (ALCH4 Project) – both grants received by Prof. Georg Wohlfahrt (University of Innsbruck). The measurements in Bautzen Reservoir and U. Spank were supported by the German Science Foundation in frame of the projects TREGATA (project number 288267759) and MEDIWA (project number 445326344). V. Stepanenko was supported by Russian Ministry of Science and Higher Education (agreement No. 075-15-2019-1621). P. Torma was supported by the by the National Research, Development and Innovation Office (grant numbers K134559 and K138176). I. Mammarella and T. Vesala acknowledge funding from ICOS-Finland (University of Helsinki). We thank Christian Wille, Sarah Waldo and Werner Eugster for providing the data. The authors declare no conflicts of interest.

Open Research

Derived quantities such as the bulk transfer coefficients are available in the open data repository Zenodo 10.5281/zenodo.6597829. Original datasets are available from the open data repositories or from the co-authors (see details in Table S1).

References

Akylas, E., Tsakos, Y., Tombrou, M., & Lalas, D. P. (2003). Considerations

on minimum friction velocity. *Quarterly Journal of the Royal Meteorological Society*, *129*(591), 1929–1943. https://doi.org/10.1256/qj.01.73Ala-Könni, J., Kohonen, K.-M., Leppäranta, M., & Mammarella, I. (2021). *Validation of turbulent heat transfer models against eddy covariance flux measurements over a seasonally ice covered lake* [Preprint]. Atmospheric sciences. https://doi.org/10.5194/gmd-2021-272Arola, A. (1999). Parameterization of Turbulent and Mesoscale Fluxes for Heterogeneous Surfaces. *Journal of the Atmospheric Sciences*, *56*(4), 584–598. https://doi.org/10.1175/1520-0469(1999)056<0584:POTAMF>2.0.CO;2Ataktürk, S. S., & Katsaros, K. B. (1999). *Wind Stress and Surface Waves Observed on Lake Washington*. *29*(4), 633–650. https://doi.org/10.1175/1520-0485(1999)029<0633:WSASWO>2.0.CO;2Babanin, A. V., & Makin, V. K. (2008). Effects of wind trend and gustiness on the sea drag: Lake George study. *Journal of Geophysical Research*, *113*(C2), C02015. https://doi.org/10.1029/2007JC004233Balsamo, G., Salgado, R., Dutra, E., Boussetta, S., Stockdale, T., & Potes, M. (2012). On the contribution of lakes in predicting near-surface temperature in a global weather forecasting model. *Tellus A: Dynamic Meteorology and Oceanography*, *64*(1), 15829. https://doi.org/10.3402/tellusa.v64i0.15829Beljaars, A. C. M. (1995). The parametrization of surface fluxes in large-scale models under free convection. *Quarterly Journal of the Royal Meteorological Society*, *121*(522), 255–270. https://doi.org/10.1002/qj.49712152203Blanken, P. D., Rouse, W. R., Culf, A. D., Spence, C., Boudreau, L. D., Jasper, J. N., Kochtubajda, B., Schertzer, W. M., Marsh, P., & Verseghy, D. (2000). Eddy covariance measurements of evaporation from Great Slave Lake, Northwest Territories, Canada. *Water Resources Research*, *36*(4), 1069–1077. https://doi.org/10.1029/1999WR900338Brutsaert, W., & Yeh, G.-T. (1970). Implications of a Type of Empirical Evaporation Formula for Lakes and Pans. *Water Resources Research*, *6*(4), 1202–1208. https://doi.org/10.1029/WR006i004p01202Burba, G. G., & Anderson, D. J. (2010). *A Brief Practical Guide to Eddy Covariance Flux Measurements: Principles and Workflow Examples for Scientific and Industrial Applications*. LI-COR Biosciences.Businger, J. A., Wyngaard, J. C., Izumi, Y., & Bradley, E. F. (1971). Flux-Profile Relationships in the Atmospheric Surface Layer. *Journal of the Atmospheric Sciences*, *28*(2), 181–189. https://doi.org/10.1175/1520-0469(1971)028<0181:FPRITA>2.0.CO;2Castelli, S. T., Ferrero, E., Anfossi, D., & Ohba, R. (2005). Turbulence closure models and their application in RAMS. *Environmental Fluid Mechanics*, *5*(1–2), 169–192. https://doi.org/10.1007/s10652-005-1596-7Changnon, S. A., & Jones, D. M. A. (1972). Review of the influences of the Great Lakes on weather. *Water Resources Research*, *8*(2), 360–371. https://doi.org/10.1029/WR008i002p00360Charnock, H. (1955). Wind stress on a water surface. *Quarterly Journal of the Royal Meteorological Society*, *81*(350), 639–640. https://doi.org/10.1002/qj.49708135027Chen, F., Zhang, C., Brett, M. T., & Nielsen, J. M. (2020). The importance of the wind-drag coefficient parameterization for hydrodynamic modeling of a large shallow lake. *Ecological Informatics*, *59*, 101106. https://doi.org/10.1016/j.ecoinf.2020.101106de Vrese, P., Schulz, J.-P., & Hagemann, S. (2016). On the Representation of

Heterogeneity in Land-Surface–Atmosphere Coupling. *Boundary-Layer Meteorology*, *160*(1), 157–183. https://doi.org/10.1007/s10546-016-0133-1DelSontro, T., Beaulieu, J. J., & Downing, J. A. (2018). Greenhouse gas emissions from lakes and impoundments: Upscaling in the face of global change. *Limnology and Oceanography Letters*, *3*(3), 64–75. https://doi.org/10.1002/lol2.10073Desai, A. R., Austin, J. A., Bennington, V., & McKinley, G. A. (2009). Stronger winds over a large lake in response to weakening air-to-lake temperature gradient. *Nature Geoscience*, *2*(12), 855–858. https://doi.org/10.1038/ngeo693Dias, N. L., & Vissotto, D. (2017). The effect of temperature-humidity similarity on Bowen ratios, dimensionless standard deviations, and mass transfer coefficients over a lake: Temperature-Humidity Similarity over a Lake. *Hydrological Processes*, *31*(2), 256–269. https://doi.org/10.1002/hyp.10925Donelan, A. (1990). Air-sea interaction. In *The Sea* (Vol. 9, pp. 239–292). Environment and Climate Change Canada.Donelan, M. (1982). The dependence of the aerodynamic drag coefficient on wave parameters. *Proc.. First Int. Conf. on Meteorology and Air-Sea Interaction of the Coastal Zone*, 381–387.Downing, J. A., Prairie, Y. T., Cole, J. J., Duarte, C. M., Tranvik, L. J., Striegl, R. G., McDowell, W. H., Kortelainen, P., Caraco, N. F., Melack, J. M., & Middelburg, J. J. (2006). The global abundance and size distribution of lakes, ponds, and impoundments. *Limnology and Oceanography*, *51*(5), 2388–2397. https://doi.org/10.4319/lo.2006.51.5.2388Edson, J. B., Jampana, V., Weller, R. A., Bigorre, S. P., Plueddemann, A. J., Fairall, C. W., Miller, S. D., Mahrt, L., Vickers, D., & Hersbach, H. (2013). On the Exchange of Momentum over the Open Ocean. *Journal of Physical Oceanography*, *43*(8), 1589–1610. https://doi.org/10.1175/JPO-D-12-0173.1Eerola, K., Rontu, L., Kourzeneva, E., Pour, H. K., & Duguay, C. (2014). Impact of partly ice-free Lake Ladoga on temperature and cloudiness in an anticyclonic winter situation – a case study using a limited area model. *Tellus A: Dynamic Meteorology and Oceanography*, *66*(1), 23929. https://doi.org/10.3402/tellusa.v66.23929Esau, I., Tolstykh, M., Fadeev, R., Shashkin, V., Makhnorylova, S., Miles, V., & Melnikov, V. (2018). Systematic errors in northern Eurasian short-term weather forecasts induced by atmospheric boundary layer thickness. *Environmental Research Letters*, *13*(12), 125009. https://doi.org/10.1088/1748-9326/aaecfbFairall, C. W., Bradley, E. F., Hare, J. E., Grachev, A. A., & Edson, J. B. (2003). Bulk Parameterization of Air–Sea Fluxes: Updates and Verification for the COARE Algorithm. *Journal of Climate*, *16*(4), 571–591. https://doi.org/10.1175/1520-0442(2003)016<0571:BPOASF>2.0.CO;2Fairall, C. W., Bradley, E. F., Rogers, D. P., Edson, J. B., & Young, G. S. (1996). Bulk parameterization of air-sea fluxes for Tropical Ocean-Global Atmosphere Coupled-Ocean Atmosphere Response Experiment. *Journal of Geophysical Research: Oceans*, *101*(C2), 3747–3764. https://doi.org/10.1029/95JC03205Foken, T. (2008). *Micrometeorology*. Springer Berlin Heidelberg. https://doi.org/10.1007/978-3-540-74666-9Foken, T., Aubinet, M., & Leuning, R. (2012). The Eddy Covariance Method. In M. Aubinet, T. Vesala, & D. Papale (Eds.), *Eddy Covariance* (pp. 1–19). Springer Netherlands. https://doi.org/10.1007/978-94-007-2351-1_1Foken, T., Göckede, M., Mauder, M., Mahrt, L., Amiro, D.,

& Munger, J. W. (2004). Post-field data quality control. In *Handbook of micrometeorology: A guide for surface flux measurement and analysis* (pp. 181–208).Foken, Th., & Wichura, B. (1996). Tools for quality assessment of surface-based flux measurements. *Agricultural and Forest Meteorology*, *78*(1–2), 83–105. https://doi.org/10.1016/0168-1923(95)02248-1Fujisaki-Manome, A., Mann, G. E., Anderson, E. J., Chu, P. Y., Fitzpatrick, L. E., Benjamin, S. G., James, E. P., Smirnova, T. G., Alexander, C. R., & Wright, D. M. (2020). Improvements to Lake-Effect Snow Forecasts Using a One-Way Air–Lake Model Coupling Approach. *Journal of Hydrometeorology*, *21*(12), 2813–2828. https://doi.org/10.1175/JHM-D-20-0079.1Garratt, J. (1994). Review: The atmospheric boundary layer. *Earth-Science Reviews*, *37*(1–2), 89–134. https://doi.org/10.1016/0012-8252(94)90026-4Garratt, J. R. (1977). Review of Drag Coefficients over Oceans and Continents. *Monthly Weather Review*, *105*(7), 915–929. https://doi.org/10.1175/1520-0493(1977)105<0915:RODCOO>2.0.CO;2Geernaert, G. L. (1990). Bulk Parameterizations for the Wind Stress and Heat Fluxes. In G. L. Geernaert & W. L. Plant (Eds.), *Surface Waves and Fluxes* (pp. 91–172). Springer Netherlands. https://doi.org/10.1007/978-94-009-2069-9_5Glazunov, A. V., & Stepanenko, V. M. (2015). Large-eddy simulation of stratified turbulent flows over heterogeneous landscapes. *Izvestiya, Atmospheric and Oceanic Physics*, *51*(4), 351–361. https://doi.org/10.1134/S0001433815040027Godfrey, J. S., & Beljaars, A. C. M. (1991). On the turbulent fluxes of buoyancy, heat and moisture at the air-sea interface at low wind speeds. *Journal of Geophysical Research*, *96*(C12), 22043. https://doi.org/10.1029/91JC02015Golub, M., Desai, A. R., Vesala, T., Mammarella, I., Ojala, A., Bohrer, G., Weyhenmeyer, G. A., Blanken, P. D., Eugster, W., Koebsch, F., Chen, J., Czajkowski, K. P., Deshmukh, C., Guérin, F., Heiskanen, J. J., Humphreys, E. R., Jonsson, A., Karlsson, J., Kling, G. W., … Xiao, W. (2021). *New insights into diel to interannual variation in carbon dioxide emissions from lakes and reservoirs* [Preprint]. Environmental Sciences. https://doi.org/10.1002/essoar.10507313.1Grachev, A. A., Fairall, C. W., & Larsen, S. E. (1998). On the Determination of the Neutral Drag Coefficient in the Convective Boundary Layer. *Boundary-Layer Meteorology*, *86*(2), 257–278. https://doi.org/10.1023/A:1000617300732Graf, W. H., Merzi, N., & Perrinjaquet, C. (1984). Aerodynamic drag: Measured at a nearshore platform on lake of Geneva. *Archives for Meteorology, Geophysics, and Bioclimatology Series A*, *33*(2–3), 151–173. https://doi.org/10.1007/BF02257722Grant, L., Vanderkelen, I., Gudmundsson, L., Tan, Z., Perroud, M., Stepanenko, V. M., Debolskiy, A. V., Droppers, B., Janssen, A. B. G., Woolway, R. I., Choulga, M., Balsamo, G., Kirillin, G., Schewe, J., Zhao, F., del Valle, I. V., Golub, M., Pierson, D., Marcé, R., … Thiery, W. (2021). Attribution of global lake systems change to anthropogenic forcing. *Nature Geoscience*, *14*(11), 849–854. https://doi.org/10.1038/s41561-021-00833-xGuseva, S., Casper, P., Sachs, T., Spank, U., & Lorke, A. (2021). Energy Flux Paths in Lakes and Reservoirs. *Water*, *13*(22), 3270. https://doi.org/10.3390/w13223270Harbeck, G. E. (1962). *A Practical Field Technique for Measuring Reservoir Evaporation Utilizing Mass-Transfer Theory.* 101–105.Heikinheimo, M., Kangas,

M., Tourula, T., Venäläinen, A., & Tattari, S. (1999). Momentum and heat fluxes over lakes Tämnaren and Råksjö determined by the bulk-aerodynamic and eddy-correlation methods. *Agricultural and Forest Meteorology*, *98–99*, 521–534. https://doi.org/10.1016/S0168-1923(99)00121-5Hicks, B. B. (1972). Some evaluations of drag and bulk transfer coefficients over water bodies of different sizes. *Boundary-Layer Meteorology*, *3*(2), 201–213. https://doi.org/10.1007/BF02033919Högström, U. (1988). Non-Dimensional Wind and Temperature Profiles in the Atmospheric Surface Layer: A Re-Evaluation. In B. B. Hicks (Ed.), *Topics in Micrometeorology. A Festschrift for Arch Dyer* (pp. 55–78). Springer Netherlands. https://doi.org/10.1007/978-94-009-2935-7_6Hwang, P. A. (2004). Influence of wavelength on the parameterization of drag coefficient and surface roughness. *Journal of Oceanography*, *60*(5), 835–841. https://doi.org/10.1007/s10872-005-5776-3Jöhnk, K. D., Huisman, J., Sharples, J., Sommeijer, B., Visser, P. M., & Stroom, J. M. (2008). Summer heatwaves promote blooms of harmful cyanobacteria: HEATWAVES PROMOTE HARMFUL CYANOBACTERIA. *Global Change Biology*, *14*(3), 495–512. https://doi.org/10.1111/j.1365-2486.2007.01510.xKaimal, J. C., & Finnigan, J. J. (1994). *Atmospheric Boundary Layer Flows: Their Structure and Measurement*. Oxford University Press. https://doi.org/10.1093/oso/9780195062397.001.0001Kantha, L., & Clayson, C. (2000). *Small Scale Processes in Geophysical Fluid Flows* (1st Edition, Vol. 67). Academic Press.Kato, H., & Takahashi, H. (1981). Local Climate near the Small Lake. *Journal of Agricultural Meteorology*, *37*(1), 29–37. https://doi.org/10.2480/agrmet.37.29Kuznetsova, A., Baydakov, G., Papko, V., Kandaurov, A., Vdovin, M., Sergeev, D., & Troitskaya, Y. (2016). Field and numerical study of the wind-wave regime on the Gorky Reservoir. *GEOGRAPHY, ENVIRONMENT, SUSTAINABILITY*, *9*(2), 19–37. https://doi.org/10.15356/2071-9388_02v09_2016_02Large, W. G., & Pond, S. (1981). *Open ocean momentum flux measurements in moderate to strong winds*. *11*(3), 324–336. https://doi.org/10.1175/1520-0485(1981)011<0324:OOMFMI>2.0.CO;2Lee, X., Liu, S., Xiao, W., Wang, W., Gao, Z., Cao, C., Hu, C., Hu, Z., Shen, S., Wang, Y., Wen, X., Xiao, Q., Xu, J., Yang, J., & Zhang, M. (2014). The Taihu Eddy Flux Network: An Observational Program on Energy, Water, and Greenhouse Gas Fluxes of a Large Freshwater Lake. *Bulletin of the American Meteorological Society*, *95*(10), 1583–1594. https://doi.org/10.1175/BAMS-D-13-00136.1Lenschow, D. H., Mann, J., & Kristensen, L. (1994). How Long Is Long Enough When Measuring Fluxes and Other Turbulence Statistics? *Journal of Atmospheric and Oceanic Technology*, *11*(3), 661–673. https://doi.org/10.1175/1520-0426(1994)011<0661:HLILEW>2.0.CO;2Li, Z., Lyu, S., Zhao, L., Wen, L., Ao, Y., & Wang, S. (2016). Turbulent transfer coefficient and roughness length in a high-altitude lake, Tibetan Plateau. *Theoretical and Applied Climatology*, *124*(3–4), 723–735. https://doi.org/10.1007/s00704-015-1440-zLI-COR, Inc. (2021). *EddyPro® Software (Version 7.0)*. LI-COR. https://www.licor.com/env/support/EddyPro/home.htmlLin, W., Sanford, L. P., Suttles, S. E., & Valigura, R. (2002). Drag Coefficients with Fetch-

Limited Wind Waves*. *Journal of Physical Oceanography*, *32*(11), 3058–3074. https://doi.org/10.1175/1520-0485(2002)032<3058:DCWFLW>2.0.CO;2Liu, C., Li, Y., Gao, Z., Zhang, H., Wu, T., Lu, Y., & Zhang, X. (2020). Improvement of Drag Coefficient Calculation Under Near-Neutral Conditions in Light Winds Over land. *Journal of Geophysical Research: Atmospheres*, *125*(24). https://doi.org/10.1029/2020JD033472Ljungemyr, P., Gustafsson, N., & Omstedt, A. (1996). Parameterization of lake thermodynamics in a high-resolution weather forecasting model. *Tellus A*, *48*(5), 608–621. https://doi.org/10.1034/j.1600-0870.1996.t01-4-00002.xLükő, G., Torma, P., Krámer, T., Weidinger, T., Vecenaj, Z., & Grisogono, B. (2020). Observation of wave-driven air–water turbulent momentum exchange in a large but fetch-limited shallow lake. *Advances in Science and Research*, *17*, 175–182. https://doi.org/10.5194/asr-17-175-2020MacKay, M. D. (2019). Incorporating wind sheltering and sediment heat flux into 1-D models of small boreal lakes: A case study with the Canadian Small Lake Model V2.0. *Geoscientific Model Development*, *12*(7), 3045–3054. https://doi.org/10.5194/gmd-12-3045-2019Mammarella, I., Nordbo, A., Rannik, Ü., Haapanala, S., Levula, J., Laakso, H., Ojala, A., Peltola, O., Heiskanen, J., Pumpanen, J., & Vesala, T. (2015). Carbon dioxide and energy fluxes over a small boreal lake in Southern Finland: CO $_2$ and Energy Fluxes Over Lake. *Journal of Geophysical Research: Biogeosciences*, *120*(7), 1296–1314. https://doi.org/10.1002/2014JG002873Mammarella, I., Peltola, O., Nordbo, A., Järvi, L., & Rannik, Ü. (2016). Quantifying the uncertainty of eddy covariance fluxes due to the use ofdifferent software packages and combinations of processing steps in twocontrasting ecosystems. *Atmospheric Measurement Techniques*, *9*(10), 4915–4933. https://doi.org/10.5194/amt-9-4915-2016Mauder, M., & Foken, T. (2015). *Eddy-Covariance Software TK3*. Zenodo. https://doi.org/10.5281/ZENODO.20349Mironov, D., Heise, E., Kourzeneva, E., Ritter, B., Schneider, N., & Terzhevik, A. (2010). *Implementation of the lake parameterization scheme FLake into the numerical weather prediction model COSMO*. *15*, 218-- 230.Molod, A., Salmun, H., & Waugh, D. W. (2003). A New Look at Modeling Surface Heterogeneity: Extending Its Influence in the Vertical. *Journal of Hydrometeorology*, *4*(5), 810–825. https://doi.org/10.1175/1525-7541(2003)004<0810:ANLAMS>2.0.CO;2Monin, A. S., & Obukhov, A. M. (1954). *Basic laws of turbulent mixing in the ground layer of the atmosphere* (Vol. 151). Akad. Nauk. SSSR Geofiz. Inst. Tr.Nordbo, A., Launiainen, S., Mammarella, I., Leppäranta, M., Huotari, J., Ojala, A., & Vesala, T. (2011). Long-term energy flux measurements and energy balance over a small boreal lake using eddy covariance technique. *Journal of Geophysical Research*, *116*(D2), D02119. https://doi.org/10.1029/2010JD014542Obukhov, A. M. (1971). Turbulence in an atmosphere with a non-uniform temperature. *Boundary-Layer Meteorology*, *2*(1), 7–29. https://doi.org/10.1007/BF00718085Oke, T. R. (1987). *Boundary Layer Climates* (2nd Edition). Methuen.Panin, G. N., Nasonov, A. E., & Foken, T. (2006). Evaporation and heat exchange of a body of water with the atmosphere in a shallow zone. *Izvestiya, Atmospheric and Oceanic Physics*, *42*(3),

337–352. https://doi.org/10.1134/S0001433806030078Paulson, C. A. (1970). *The mathematical representation of wind speed and temperature profiles in the unstable atmospheric surface layer*. *9*(6), 857–861. https://doi.org/10.1175/1520-0450(1970)009<0857:TMROWS>2.0.CO;2Pawlowicz, R. (2020). *M_Map: A mapping package for MATLAB* (1.4m) [Computer software]. available online at www.eoas.ubc.ca/~rich/map.htmlRead, J. S., Hamilton, D. P., Desai, A. R., Rose, K. C., MacIntyre, S., Lenters, J. D., Smyth, R. L., Hanson, P. C., Cole, J. J., Staehr, P. A., Rusak, J. A., Pierson, D. C., Brookes, J. D., Laas, A., & Wu, C. H. (2012). Lake-size dependency of wind shear and convection as controls on gas exchange. *Geophysical Research Letters*, *39*(9). https://doi.org/10.1029/2012GL051886Read, J. S., Winslow, L. A., Hansen, G. J. A., Van Den Hoek, J., Hanson, P. C., Bruce, L. C., & Markfort, C. D. (2014). Simulating 2368 temperate lakes reveals weak coherence in stratification phenology. *Ecological Modelling*, *291*, 142–150. https://doi.org/10.1016/j.ecolmodel.2014.07.029Rosentreter, J. A., Borges, A. V., Deemer, B. R., Holgerson, M. A., Liu, S., Song, C., Melack, J., Raymond, P. A., Duarte, C. M., Allen, G. H., Olefeldt, D., Poulter, B., Battin, T. I., & Eyre, B. D. (2021). Half of global methane emissions come from highly variable aquatic ecosystem sources. *Nature Geoscience*, *14*(4), 225–230. https://doi.org/10.1038/s41561-021-00715-2Sahlée, E., Rutgersson, A., Podgrajsek, E., & Bergström, H. (2014). Influence from Surrounding Land on the Turbulence Measurements Above a Lake. *Boundary-Layer Meteorology*, *150*(2), 235–258. https://doi.org/10.1007/s10546-013-9868-0Salgado, R., & Le Mogne, P. (2010). *Coupling the FLake model to the Surfex externalized surface model*. *15*, 231-- 244.Schlichting, H. (1968). *Boundary-Layer Theory* (6th Edition). McGraw-Hill Book Company.Simon, A. (1997). *Turbulent mixing in the surface boundary layer of lakes* [Dissertation No 12272]. Swiss Federal Institute of Technology.Smith, S. D., Fairall, C. W., Geernaert, G. L., & Hasse, L. (1996). Air-sea fluxes: 25 years of progress. *Boundary-Layer Meteorology*, *78*(3–4), 247–290. https://doi.org/10.1007/BF00120938Spank, U., Hehn, M., Keller, P., Koschorreck, M., & Bernhofer, C. (2020). A Season of Eddy-Covariance Fluxes Above an Extensive Water Body Based on Observations from a Floating Platform. *Boundary-Layer Meteorology*, *174*(3), 433–464. https://doi.org/10.1007/s10546-019-00490-zStepanenko, V., Jöhnk, K. D., Machulskaya, E., Perroud, M., Subin, Z., Nordbo, A., Mammarella, I., & Mironov, D. (2014). Simulation of surface energy fluxes and stratification of a small boreal lake by a set of one-dimensional models. *Tellus A: Dynamic Meteorology and Oceanography*, *66*(1), 21389. https://doi.org/10.3402/tellusa.v66.21389Strub, T. P., & Powell, T. M. (1987). The exchange coefficients for latent and sensible heat flux over lakes: Dependence upon atmospheric stability. *Boundary-Layer Meteorology*, *40*(4), 349–362. https://doi.org/10.1007/BF00116102Stull, R. B. (Ed.). (1988). *An Introduction to Boundary Layer Meteorology*. Springer Netherlands. https://doi.org/10.1007/978-94-009-3027-8Sun, J., Lenschow, D. H., Mahrt, L., Crawford, T. L., Davis, K. J., Oncley, S. P., MacPherson, J. I., Wang, Q., Dobosy, R. J., & Desjardins, R. L. (1997). Lake-induced atmospheric circulations

during BOREAS. *Journal of Geophysical Research: Atmospheres*, *102*(D24), 29155–29166. https://doi.org/10.1029/97JD01114Sun, X.-M., Zhu, Z.-L., Wen, X.-F., Yuan, G.-F., & Yu, G.-R. (2006). The impact of averaging period on eddy fluxes observed at ChinaFLUX sites. *Agricultural and Forest Meteorology*, *137*(3–4), 188–193. https://doi.org/10.1016/j.agrformet.2006.02.012Thiery, W., Davin, E. L., Seneviratne, S. I., Bedka, K., Lhermitte, S., & van Lipzig, N. P. M. (2016). Hazardous thunderstorm intensification over Lake Victoria. *Nature Communications*, *7*(1), 12786. https://doi.org/10.1038/ncomms12786Vesala, T., Huotari, J., Rannik, Ü., Suni, T., Smolander, S., Sogachev, A., Launiainen, S., & Ojala, A. (2006). Eddy covariance measurements of carbon exchange and latent and sensible heat fluxes over a boreal lake for a full open-water period. *Journal of Geophysical Research*, *111*(D11), D11101. https://doi.org/10.1029/2005JD006365Vickers, D., & Mahrt, L. (1997). Fetch Limited Drag Coefficients. *Boundary-Layer Meteorology*, *85*(1), 53–79. https://doi.org/10.1023/A:1000472623187von Salzen, K., M. Claussen, M., & Schlünzen, K. H. (1996). Anwendung des Konzepts der Blendhöhe zur Berechnung von bodennahen Flüssen in einem mesoskaligen Modell. *Meteorologische Zeitschrift*, *5*(2), 60–66. https://doi.org/10.1127/metz/5/1996/60Wei, Z., Miyano, A., & Sugita, M. (2016). Drag and Bulk Transfer Coefficients Over Water Surfaces in Light Winds. *Boundary-Layer Meteorology*, *160*(2), 319–346. https://doi.org/10.1007/s10546-016-0147-8Woolway, R. I., & Merchant, C. J. (2019). Worldwide alteration of lake mixing regimes in response to climate change. *Nature Geoscience*, *12*(4), 271–276. https://doi.org/10.1038/s41561-019-0322-xWoolway, R. I., Verburg, P., Lenters, J. D., Merchant, C. J., Hamilton, D. P., Brookes, J., Eyto, E., Kelly, S., Healey, N. C., Hook, S., Laas, A., Pierson, D., Rusak, J. A., Kuha, J., Karjalainen, J., Kallio, K., Lepistö, A., & Jones, I. D. (2018). Geographic and temporal variations in turbulent heat loss from lakes: A global analysis across 45 lakes. *Limnology and Oceanography*, *63*(6), 2436–2449. https://doi.org/10.1002/lno.10950Woolway, R. I., Verburg, P., Merchant, C. J., Lenters, J. D., Hamilton, D. P., Brookes, J., Kelly, S., Hook, S., Laas, A., Pierson, D., Rimmer, A., Rusak, J. A., & Jones, I. D. (2017). Latitude and lake size are important predictors of over-lake atmospheric stability: Atmospheric Stability Above Lakes. *Geophysical Research Letters*, *44*(17), 8875–8883. https://doi.org/10.1002/2017GL073941Wu, J. (1988). Wind-Stress Coefficients at Light Winds. *Journal of Atmospheric and Oceanic Technology*, *5*(6), 885–888. https://doi.org/10.1175/1520-0426(1988)005<0885:WSCALW>2.0.CO;2Wu, J. (1994). The sea surface is aerodynamically rough even under light winds. *Boundary-Layer Meteorology*, *69*(1–2), 149–158. https://doi.org/10.1007/BF00713300Wu, L., Breivik, Ø., & Rutgersson, A. (2019). Ocean-Wave-Atmosphere Interaction Processes in a Fully Coupled Modeling System. *Journal of Advances in Modeling Earth Systems*, *11*(11), 3852–3874. https://doi.org/10.1029/2019MS001761Wüest, A., & Lorke, A. (2003). Small-Scale Hydrodynamics in Lakes. *Annual Review of Fluid Mechanics*, *35*(1), 373–412. https://doi.org/10.1146/annurev.fluid.35.101101.161220Xiao, W., Liu, S., Wang, W., Yang, D., Xu, J., Cao, C., Li, H., & Lee, X. (2013). Transfer Coefficients of Momentum, Heat and Water Vapour in the Atmo-

spheric Surface Layer of a Large Freshwater Lake. *Boundary-Layer Meteorology*, *148*(3), 479–494. https://doi.org/10.1007/s10546-013-9827-9Zhu, P., & Furst, J. (2013). On the parameterization of surface momentum transport via drag coefficient in low-wind conditions. *Geophysical Research Letters*, *40*(11), 2824–2828. https://doi.org/10.1002/grl.50518Zilitinkevich, S., & Calanca, P. (2010). An extended similarity theory for the stably stratified atmospheric surface layer. *Quarterly Journal of the Royal Meteorological Society*, *126*(566), 1913–1923. https://doi.org/10.1002/qj.49712656617

References from Supporting Information

Armani, F. A. S., Dias, N. L., & Damázio, J. M. (2020). Eddy-covariance CO2 fluxes over Itaipu lake, southern Brazil. *RBRH*, *25*, e43. https://doi.org/10.1590/2318-0331.252020200060Demarty, M., Bastien, J., & Tremblay, A. (2011). Annual follow-up of gross diffusive carbon dioxide and methane emissions from a boreal reservoir and two nearby lakes in Québec, Canada. *Biogeosciences*, *8*(1), 41–53. https://doi.org/10.5194/bg-8-41-2011Desai, A. (2018). *AmeriFlux AmeriFlux US-Pnp Lake Mendota, Picnic Point Site* [Data set]. AmeriFlux; University of Wisconsin Madison. https://doi.org/10.17190/AMF/1433376Deshmukh, C., Serça, D., Delon, C., Tardif, R., Demarty, M., Jarnot, C., Meyerfeld, Y., Chanudet, V., Guédant, P., Rode, W., Descloux, S., & Guérin, F. (2014). Physical controls on CH₄ emissions from a newly flooded subtropical freshwater hydroelectric reservoir: Nam Theun 2. *Biogeosciences*, *11*(15), 4251–4269. https://doi.org/10.5194/bg-11-4251-2014Eugster, W. (2003). CO $_2$ exchange between air and water in an Arctic Alaskan and midlatitude Swiss lake: Importance of convective mixing. *Journal of Geophysical Research*, *108*(D12), 4362. https://doi.org/10.1029/2002JD002653Eugster, W., DelSontro, T., Shaver, G. R., & Kling, G. W. (2020). Interannual, summer, and diel variability of CH $_4$ and CO $_2$ effluxes from Toolik Lake, Alaska, during the ice-free periods 2010–2015. *Environmental Science: Processes & Impacts*, 10.1039.D0EM00125B. https://doi.org/10.1039/D0EM00125BEugster, W., DelSontro, T., & Sobek, S. (2011). *Eddy covariance flux measurements confirm extreme CH₄ emissions from a Swiss hydropower reservoir and resolve their short-term variability* [Preprint]. Biogeochemistry: Greenhouse Gases. https://doi.org/10.5194/bgd-8-5019-2011Foken, T., Leuning, R., Oncley, S. R., Mauder, M., & Aubinet, M. (2012). Corrections and Data Quality Control. In M. Aubinet, T. Vesala, & D. Papale (Eds.), *Eddy Covariance* (pp. 85–131). Springer Netherlands. https://doi.org/10.1007/978-94-007-2351-1_4Franz, D., Mammarella, I., Boike, J., Kirillin, G., Vesala, T., Bornemann, N., Larmanou, E., Langer, M., & Sachs, T. (2018). Lake-Atmosphere Heat Flux Dynamics of a Thermokarst Lake in Arctic Siberia. *Journal of Geophysical Research: Atmospheres*, *123*(10), 5222–5239. https://doi.org/10.1029/2017JD027751Golub, M., Desai, A. R., Vesala, T., Mammarella, I., Ojala, A., Bohrer, G., Weyhenmeyer, G. A., Blanken, P. D., Eugster, W., Koebsch, F., Chen, J., Czajkowski, K. P., Deshmukh, C., Guérin, F., Heiskanen, J. J., Humphreys, E. R., Jonsson, A., Karlsson, J., Kling, G. W.,

… Xiao, W. (2021a). *New insights into diel to interannual variation in carbon dioxide emissions from lakes and reservoirs* [Preprint]. Environmental Sciences. https://doi.org/10.1002/essoar.10507313.1Golub, M., Desai, A. R., Vesala, T., Mammarella, I., Ojala, A., Bohrer, G., Weyhenmeyer, G. A., Blanken, P. D., Eugster, W., Koebsch, F., Chen, J., Czajkowski, K. P., Deshmukh, C., Guérin, F., Heiskanen, J. J., Humphreys, E. R., Jonsson, A., Karlsson, J., Kling, G. W., … Xiao, W. (2021b). *New insights into diel to interannual variation in carbon dioxide emissions from lakes and reservoirs* [Preprint]. Environmental Sciences. https://doi.org/10.1002/essoar.10507313.1Golub, M., Desai, A. R., Vesala, T., Mammarella, I., Ojala, A., Bohrer, G., Weyhenmeyer, G., Blanken, P., Eugster, W., Franz, D., Koebsch, F., Chen, J., Czajkowski, K., Deshmukh, C. S., Elbers, J., Friborg, T., Glatzel, S., Guerin, F., Heiskanen, J., … Xiao, W. (2022). *Half-hourly gap-filled Northern Hemisphere lake and reservoir carbon flux and micrometeorology, 2006—2015* [Data set]. Environmental Data Initiative. https://doi.org/10.6073/PASTA/87A35CA843D8739D75882520C724E99EGuseva, S., Casper, P., Sachs, T., Spank, U., & Lorke, A. (2021). Energy Flux Paths in Lakes and Reservoirs. *Water*, *13*(22), 3270. https://doi.org/10.3390/w13223270Han, B. (2020). *Eddy covariance data in Ngoring Lake in Tibet from 2011 to 2013* [Data set]. Harvard Dataverse. https://doi.org/10.7910/DVN/SRIAYJHan, B., Meng, X., Yang, Q., Wu, R., Lv, S., Li, Z., Wang, X., Li, Y., & Yu, L. (2020). Connections Between Daily Surface Temperature Contrast and CO $_2$ Flux Over a Tibetan Lake: A Case Study of Ngoring Lake. *Journal of Geophysical Research: Atmospheres*, *125*(6). https://doi.org/10.1029/2019JD032277Heiskanen, J. J., Mammarella, I., Ojala, A., Stepanenko, V., Erkkilä, K., Miettinen, H., Sandström, H., Eugster, W., Leppäranta, M., Järvinen, H., Vesala, T., & Nordbo, A. (2015). Effects of water clarity on lake stratification and lake-atmosphere heat exchange. *Journal of Geophysical Research: Atmospheres*, *120*(15), 7412–7428. https://doi.org/10.1002/2014JD022938Iwata, H., Hirata, R., Takahashi, Y., Miyabara, Y., Itoh, M., & Iizuka, K. (2018). Partitioning Eddy-Covariance Methane Fluxes from a Shallow Lake into Diffusive and Ebullitive Fluxes. *Boundary-Layer Meteorology*, *169*(3), 413–428. https://doi.org/10.1007/s10546-018-0383-1Iwata, H., Nakazawa, K., Sato, H., Itoh, M., Miyabara, Y., Hirata, R., Takahashi, Y., Tokida, T., & Endo, R. (2020). Temporal and spatial variations in methane emissions from the littoral zone of a shallow mid-latitude lake with steady methane bubble emission areas. *Agricultural and Forest Meteorology*, *295*, 108184. https://doi.org/10.1016/j.agrformet.2020.108184Jammet, M., Dengel, S., Kettner, E., Parmentier, F.-J. W., Wik, M., Crill, P., & Friborg, T. (2017). Year-round CH₄ and CO₂ flux dynamics in two contrasting freshwater ecosystems of the subarctic. *Biogeosciences*, *14*(22), 5189–5216. https://doi.org/10.5194/bg-14-5189-2017Jansen, J., Thornton, B. F., Jammet, M. M., Wik, M., Cortés, A., Friborg, T., MacIntyre, S., & Crill, P. M. (2019). Climate-Sensitive Controls on Large Spring Emissions of CH $_4$ and CO $_2$ From Northern Lakes. *Journal of Geophysical Research: Biogeosciences*, *124*(7), 2379–2399.

https://doi.org/10.1029/2019JG005094Li, X., Yang, X., Ma, Y., Hu, G., Hu, X., Wu, X., Wang, P., Huang, Y., Cui, B., & Wei, J. (2018). Qinghai Lake Basin Critical Zone Observatory on the Qinghai-Tibet Plateau. *Vadose Zone Journal*, *17*(1), 180069. https://doi.org/10.2136/vzj2018.04.0069Li, X.-Y., Ma, Y.-J., Huang, Y.-M., Hu, X., Wu, X.-C., Wang, P., Li, G.-Y., Zhang, S.-Y., Wu, H.-W., Jiang, Z.-Y., Cui, B.-L., & Liu, L. (2016). Evaporation and surface energy budget over the largest high-altitude saline lake on the Qinghai-Tibet Plateau: WATER AND ENERGY FLUX OVER QINGHAI LAKE. *Journal of Geophysical Research: Atmospheres*, *121*(18), 10,470-10,485. https://doi.org/10.1002/2016JD025027LI-COR, Inc. (2021). *EddyPro® Software (Version 7.0)*. LI-COR. https://www.licor.com/env/support/EddyPro/home.htmlLiu, C., Li, Y., Gao, Z., Zhang, H., Wu, T., Lu, Y., & Zhang, X. (2020). Improvement of Drag Coefficient Calculation Under Near-Neutral Conditions in Light Winds Over land. *Journal of Geophysical Research: Atmospheres*, *125*(24). https://doi.org/10.1029/2020JD033472Liu, H., Zhang, Y., Liu, S., Jiang, H., Sheng, L., & Williams, Q. L. (2009). Eddy covariance measurements of surface energy budget and evaporation in a cool season over southern open water in Mississippi. *Journal of Geophysical Research*, *114*(D4), D04110. https://doi.org/10.1029/2008JD010891Lohila, A., Tuovinen, J. P., Hatakka, J., Aurela, M., Vuorenmaa, J., Haakana, M., & Laurila, T. (2015). *Carbon dioxide and energy fluxes over a northern boreal lake*. *20*(4), 474–488.Lükő, G., Torma, P., Krámer, T., Weidinger, T., Vecenaj, Z., & Grisogono, B. (2020). Observation of wave-driven air–water turbulent momentum exchange in a large but fetch-limited shallow lake. *Advances in Science and Research*, *17*, 175–182. https://doi.org/10.5194/asr-17-175-2020Lükő, G., Torma, P., & Weidinger, T. (2022). Intra-Seasonal and Intra-Annual Variation of the Latent Heat Flux Transfer Coefficient for a Freshwater Lake. *Atmosphere*, *13*(2), 352. https://doi.org/10.3390/atmos13020352Mammarella, I., Nordbo, A., Rannik, Ü., Haapanala, S., Levula, J., Laakso, H., Ojala, A., Peltola, O., Heiskanen, J., Pumpanen, J., & Vesala, T. (2015). Carbon dioxide and energy fluxes over a small boreal lake in Southern Finland: CO_2 and Energy Fluxes Over Lake. *Journal of Geophysical Research: Biogeosciences*, *120*(7), 1296–1314. https://doi.org/10.1002/2014JG002873Mauder, M., & Foken, T. (2015). *Eddy-Covariance Software TK3*. Zenodo. https://doi.org/10.5281/ZENODO.20349Morin, T. H., Rey-Sánchez, A. C., Vogel, C. S., Matheny, A. M., Kenny, W. T., & Bohrer, G. (2018). Carbon dioxide emissions from an oligotrophic temperate lake: An eddy covariance approach. *Ecological Engineering*, *114*, 25–33. https://doi.org/10.1016/j.ecoleng.2017.05.005Nordbo, A., Launiainen, S., Mammarella, I., Leppäranta, M., Huotari, J., Ojala, A., & Vesala, T. (2011). Long-term energy flux measurements and energy balance over a small boreal lake using eddy covariance technique. *Journal of Geophysical Research*, *116*(D2), D02119. https://doi.org/10.1029/2010JD014542Panin, G. N., Nasonov, A. E., & Foken, T. (2006). Evaporation and heat exchange of a body of water with the atmosphere in a shallow zone. *Izvestiya, Atmospheric and Oceanic Physics*, *42*(3), 337–352. https://doi.org/10.1134/S0001433806030078Podgrajsek, E., Sahlée, E., Bastviken, D., Holst, J., Lindroth, A., Tranvik, L., & Rut-

gersson, A. (2014). Comparison of floating chamber and eddy covariance measurements of lake greenhouse gas fluxes. *Biogeosciences*, *11*(15), 4225–4233. https://doi.org/10.5194/bg-11-4225-2014Sahlée, E., Rutgersson, A., Podgrajsek, E., & Bergström, H. (2014). Influence from Surrounding Land on the Turbulence Measurements Above a Lake. *Boundary-Layer Meteorology*, *150*(2), 235–258. https://doi.org/10.1007/s10546-013-9868-0Salgado, R., Potes, M., Mammarella, I., & Provenzale, M. (2016). *Measurements of Mass, Momentum and Energy fluxes over an ice/snow covered lake*. EGU.Scholz, K., Ejarque, E., Hammerle, A., Kainz, M., Schelker, J., & Wohlfahrt, G. (2021). Atmospheric CO $_2$ Exchange of a Small Mountain Lake: Limitations of Eddy Covariance and Boundary Layer Modeling Methods in Complex Terrain. *Journal of Geophysical Research: Biogeosciences*, *126*(7). https://doi.org/10.1029/2021JG006286Schubert, C. J., Diem, T., & Eugster, W. (2012). Methane Emissions from a Small Wind Shielded Lake Determined by Eddy Covariance, Flux Chambers, Anchored Funnels, and Boundary Model Calculations: A Comparison. *Environmental Science & Technology*, *46*(8), 4515–4522. https://doi.org/10.1021/es203465xShao, C., Chen, J., Stepien, C. A., Chu, H., Ouyang, Z., Bridgeman, T. B., Czajkowski, K. P., Becker, R. H., & John, R. (2015). Diurnal to annual changes in latent, sensible heat, and CO $_2$ fluxes over a Laurentian Great Lake: A case study in Western Lake Erie. *Journal of Geophysical Research: Biogeosciences*, *120*(8), 1587–1604. https://doi.org/10.1002/2015JG003025Sollberger, S., Wehrli, B., Schubert, C. J., DelSontro, T., & Eugster, W. (2017). Minor methane emissions from an Alpine hydropower reservoir based on monitoring of diel and seasonal variability. *Environmental Science: Processes & Impacts*, *19*(10), 1278–1291. https://doi.org/10.1039/C7EM00232GSpank, U., Hehn, M., Keller, P., Koschorreck, M., & Bernhofer, C. (2020). A Season of Eddy-Covariance Fluxes Above an Extensive Water Body Based on Observations from a Floating Platform. *Boundary-Layer Meteorology*, *174*(3), 433–464. https://doi.org/10.1007/s10546-019-00490-zStepanenko, V. M., Repina, I. A., Artamonov, A. Y., Gorin, S. L., Lykossov, V. N., & Kulyamin, D. V. (2018). Mid-depth temperature maximum in an estuarine lake. *Environmental Research Letters*, *13*(3), 035006. https://doi.org/10.1088/1748-9326/aaad75Waldo, S., Beaulieu, J. J., Barnett, W., Balz, D. A., Vanni, M. J., Williamson, T., & Walker, J. T. (2021). Temporal trends in methane emissions from a small eutrophic reservoir: The key role of a spring burst. *Biogeosciences*, *18*(19), 5291–5311. https://doi.org/10.5194/bg-18-5291-2021Woolway, R. I., Verburg, P., Lenters, J. D., Merchant, C. J., Hamilton, D. P., Brookes, J., Eyto, E., Kelly, S., Healey, N. C., Hook, S., Laas, A., Pierson, D., Rusak, J. A., Kuha, J., Karjalainen, J., Kallio, K., Lepistö, A., & Jones, I. D. (2018). Geographic and temporal variations in turbulent heat loss from lakes: A global analysis across 45 lakes. *Limnology and Oceanography*, *63*(6), 2436–2449. https://doi.org/10.1002/lno.10950Zhang, Z., Zhang, M., Cao, C., Wang, W., Xiao, W., Xie, C., Chu, H., Wang, J., Zhao, J., Jia, L., Liu, Q., Huang, W., Zhang, W., Lu, Y., Xie, Y., Wang, Y., Pu, Y., Hu, Y., Chen, Z., … Lee, X. (2020). *A dataset of microclimate and radiation and energy fluxes*

from the Lake Taihu Eddy Flux Network [Data set]. Harvard Dataverse. https://doi.org/10.7910/DVN/HEWCWM

The Journal of Geophysical Research: Atmospheres

Supporting Information for

Bulk Transfer Coefficients Estimated from Eddy-Covariance Measurements Over Lakes and Reservoirs

S. Guseva[1], F. Armani[2], A. R. Desai[3], N. L. Dias[4], T. Friborg[5], H. Iwata[6], J. Jansen[7,8], G. Lükő[9], I. Mammarella[10], I. Repina[11,12], A. Rutgersson[13], T. Sachs[14], K. Scholz[15], U. Spank[16], V. Stepanenko[12,17,18], P. Torma[9], T. Vesala[10,19], and A. Lorke[1]

[1] Institute for Environmental Sciences, University of Koblenz-Landau, Landau, Germany.
[2] Federal University of Paraná, Curitiba, PR, Brasil.
[3] Department of Atmospheric and Oceanic Sciences, University of Wisconsin-Madison, Madison, WI, USA.
[4] Department of Environmental Engineering, Federal University of Paraná, Curitiba, PR, Brasil.
[5] Department of Geosciences and Natural Resource Management, Oester Voldgade 10, 1350 Copenhagen K, Denmark.
[6] Department of Environmental Science, Faculty of Science, Shinshu University, Matsumoto, Japan.
[7] Department of Ecology and Genetics / Limnology, Uppsala University, Uppsala, Sweden.
[8] Département des Sciences Biologiques, Groupe de Recherche Interuniversitaire en Limnologie, Université du Québec à Montréal, Montréal, QC, Canada.
[9] Department of Hydraulic and Water Resources Engineering, Budapest University of Technology and Economics, Budapest, Hungary.
[10] Institute for Atmospheric and Earth System Research/Physics, Faculty of Science, University of Helsinki, Helsinki, Finland.
[11] A.M. Obukhov Institute of Atmospheric Physics, Moscow, Russia.
[12] Research Computing Center, Lomonosov Moscow State University, Moscow, Russia.
[13] Department of Earth Sciences, Uppsala University, Uppsala, Sweden.
[14] GFZ German Research Centre for Geosciences, Potsdam, Germany.
[15] Department of Ecology, University of Innsbruck, Innsbruck, Austria.
[16] Technische Universität Dresden, Faculty of Environmental Sciences, Institute of Hydrology and Meteorology, Chair of Meteorology, PF 1117, 01735 Tharandt, Germany.
[17] Faculty of Geography, Lomonosov Moscow State University, Moscow, Russia.
[18] Moscow Center of Fundamental and Applied Mathematics.
[19] Institute for Atmospheric and Earth System Research/Forest Sciences, Faculty of Agriculture and Forestry, University of Helsinki, Finland.
Corresponding author: Sofya Guseva (guseva@uni-landau.de)

Contents of this file

Text S1
Figures S1 to S11
Tables S1

Introduction

In the supporting information, we include text S1, table S1 and figures S1-S11 which are referred to Section 2.1 “Eddy-covariance measurements”, Section 2.2 “Data filtering” and Section 3 “Results”, respectively. Text S1 describes the effect of application different filters (Section 2.2) on the data. In particular, we selected two datasets from Lake Dagow and Lake Suwa which we consider representative for all other datasets. Moreover, in this text we explore different types of averaging over all datasets. Table S1 represents a short overview of the water bodies selected for the analysis and the data sources. Figures S1-S11 provide additional results related to the bulk transfer coefficients over lakes and reservoirs, known as drag coefficient (C_{DN}), Stanton number (C_{HN}) and Dalton number (C_{EN}). Figure S1 is a support for the fact that the drag coefficient at one individual bin (wind speed of 0.5 m s^{-1}) has a log-normal distribution. In addition, it shows that different kinds of averaging of the drag coefficient do not significantly affect the results. Figure S2 demonstrates the effect of the data filtering on the values of C_{DN} for one particular dataset (as an example, Lake Dagow, Germany). Figure S3 explores the effect of removing measurements that were potentially affected by floating vegetation in Lake Suwa (Japan). Figure S4a shows C_{DN} versus wind speed at 10 m height for all lakes and reservoirs. Lake Quinghai (China), Nam Theun 2 Reservoir (Laos) and Bol’shoi Vilyui Lake (Russia) were removed as they showed much larger or lower values in comparison to other water bodies of similar size. We did not find a reasonable explanation for that. In comparison with Figure 2a, Figure S4a shows less variability between the lakes. Figure S4b explores the difference between the Stanton numbers considering various types of water surface temperature: the skin temperature, the water temperature at some arbitrary depth or the mixture of both. Figure S5 provides all estimates of the transfer coefficients for the water bodies where obvious outliers are included. Figure S6 helps to understand the effect of the atmospheric stability on the transfer coefficients at wind speeds below 3 m s^{-1}. Figure S7 shows the fitting of the empirical function proposed for the measurements above the land for the Stanton and Dalton numbers. Figures S8, S10 demonstrate the relationship between the transfer coefficients and lake characteristics, including maximum fetch, maximum and mean water depth, and lake surface area. Figure S10 shows the dependence of the transfer coefficients on the measurement height. Figure S9 shows the results of a principal component analysis that was used to identify the possible relationship between C_{DN} and all predictors. Figure S11 provides evidence for the increase of the averaged wind speed with the increase of the lake surface area.

Text S1. Effect of data filtering and data averaging

Before analyzing the transfer coefficients for the combined datasets, we looked at data for each individual lake or reservoir. As a first step, we analyzed the dependence of the drag coefficient on U_{10}. It was apparent that the drag coefficients C_D (Eq. 2a) within individual wind speed intervals (0.5 m s^{-1} bin size) were nearly log-normally distributed. The Shapiro-Wilk test for logarithmically transformed data confirmed a normal distribution at a standard significance level of 0.05 for most of the bins (the example for one individual bin is shown for Lake Balaton, Hungary Figure S1a). The normalization of the drag coefficient to neutral atmospheric stability (C_{DN}) produced outliers (mainly for stable conditions), which affected the test results, but the distribution was still near log-normal. For our analysis, we consider bin-averaging of log-transformed data as an adequate measure to quantify the relation between the drag coefficient and wind speed. Some previous studies reported the median values of the drag coefficient (DeCosmo et al., 1996; Fairall et al., 2003), which are almost identical to the log-averaged values.

As there was no widely accepted way of presenting the transfer coefficients and their dependence on wind speed, we tested several statistical metrics. At first, we considered two types of representation of the transfer coefficients: the first way was to combine the data from all water bodies in each bin to estimate the mean value, logarithmic mean and median values. In the second approach, we calculated the same metrics but for already logarithmically bin averaged C_{DN} for each lake or reservoir. We did not consider arithmetic mean for the first method as the outliers strongly affected it. We found that the choice of other statistical metrics was not important due to the fact that, for example, the average percentage difference between the median of the first method (resulted in the lowest values of C_{DN}) and the standard mean of the second method (resulted in the highest values of C_{DN}) was around 20% (Figure S1b). We consider the second method and the logarithmic mean for further analysis as we observed near logarithmic distribution of the data in each bin.

To demonstrate the effect of data filtering (Section 2.2), we examined the longest dataset available to us, collected at the Lake Dagow site (Figure S2). The effects of applying the filters described below were nearly identical for any other dataset. Without any filtering, C_{DN} is characterized by large scatter, particularly, at low wind speeds (< 4 m s^{-1}) (Figure S2a). 3% of these data has been discarded after applying the quality check flags for unacceptable data. Removing wind directions (< 60°; > 90° and < 210; > 270°, see Table S1), considering the elongated shape of the lake, resulted in a slight decrease of the bin-averaged C_{DN}, except for the highest wind speed of 10 m s^{-1} (however, less data in bins were available there). A similar effect could be observed when the periods with ice cover were removed (Figure S2d). The bin-averaged C_{DN} appeared to be unaffected by removal of events with precipitation (Figure S2e). Removing data with $u_* < 0.05$ m s^{-1} resulted in increase of the bin-averaged C_{DN} at low wind speeds. In the case of Lake Dagow, C_{DN} for the first bin (U_{10} = 0-0.5 m s^{-1}) was a factor of 1.6 higher in comparison to C_{DN} without the u_* filter (Figure S2f). This selected threshold for the u_* filter is reported in literature, but is considered as arbitrary. Higher and lower values of this threshold result in higher and lower C_{DN} at low wind speeds. Following common practice, we applied the threshold of 0.05 m s^{-1} in the following analysis for all datasets. In general, the resulting filtered bin-averaged C_{DN} increased with decreasing wind speed at low wind speeds and remained at a relatively constant value of $3{\cdot}10^{-3}$ at wind speeds exceeding 3 m s^{-1} with a very slight increase at 9-10 m s^{-1}.

For their analysis, Andreas et al. (2005) and Li et al. (2016) removed the data with "unreasonable" values of the surface roughness length (e.g., $z_0 > 0.3$ m). We tested this criterion using our data (Figure S2g). While at high wind speeds (> 3 m s^{-1}) an increased surface roughness length could be attributed to the increasing height of the surface gravity waves, potential mechanism causing large roughness at low wind speed (e.g., z_0>1 m for Lake Dagow), remains

unknown. Large values of z_0 has also been reported in Liu et al. (2020) for the measurements above land. Using this criterion to filter the data seemed to be inappropriate, as it mainly affected the drag coefficient at low wind speeds and simply cuts large values of C_{DN}. This filtering resulted in smaller bin-averaged C_{DN} at low wind speeds.

Filtering of the dataset from Lake Dagow resulted in a data reduction of approximately 73% (see details in the Table in the data repository 10.5281/zenodo.6597829 for other lakes or reservoirs). Lake Dagow is a relatively small lake (0.3 km^2) shielded with forest and may have larger scatter in the dependence of the drag coefficient on wind speed. However, we consider this example of filtering the data as representative for all other lakes and reservoirs under study as it contains most of applied filters and similar effects of filtering has been observed for other sites, as well as for C_{HN} and C_{EN}.

Removing the periods with floating vegetation on the water surface using the data from Lake Suwa did not significantly affect C_{DN} except at low wind speeds (< 2 m s^{-1}, Figure S3). Bin-averaged C_{DN} was slightly higher when applying this filter (the mean percentage difference was 16% for winds 0-2 m s^{-1}, Figure S3c).

Filtering of the datasets resulted in the total amount of filtered data ranging between 6.5 days (Lake Wohlen) and 5.3 years (Lake Taihu) with median value of 110 days for all datasets.

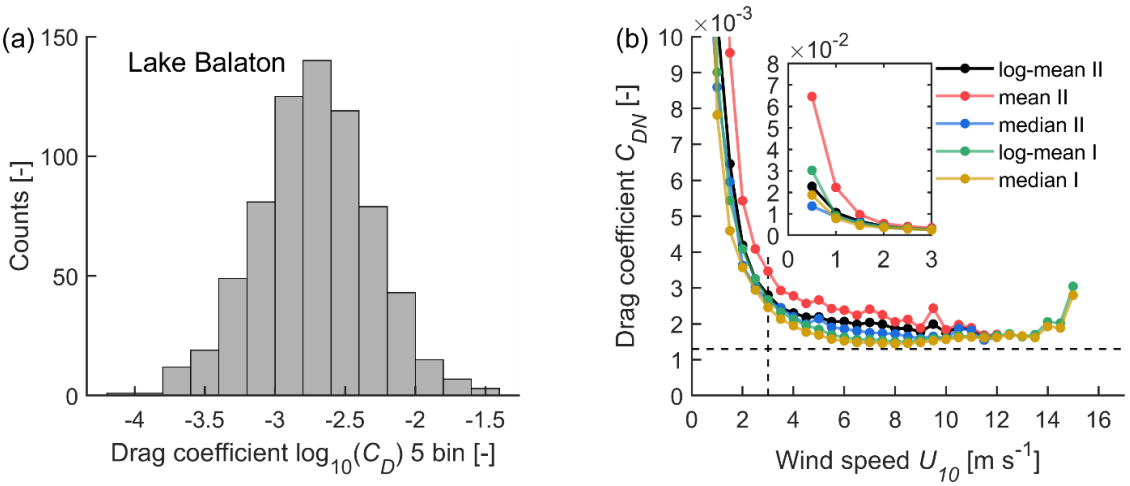

Figure S1. Histogram of log-transformed drag coefficients C_D (not accounting for atmospheric stability) for 5th bin corresponding to wind speed of 2.5 m s^{-1}. Data was collected at Lake Balaton site (Hungary, number of data points N = 694). A Shapiro-Wilk test of the log-transformed data confirmed a normal distribution at a standard significance level of 0.05. (b) Bin-averaged drag coefficients at neutral atmospheric stability (C_{DN}) estimated using the combined dataset as a function of U_{10}. Different colors refer to different averaging procedures: the first method (I) was to combine data from all water bodies in each bin of wind speeds and then estimate the logarithmic mean (black line with circles) and median (dark yellow line with circles) values (the arithmetic mean values without log-transformation are not shown because of their large scatter). For the second method (II), C_{DN} were logarithmically averaged for each lake before calculation of mean (red line and symbols), logarithmic mean (black), and median (blue) values.

The second method with logarithmic averaging was considered for further analysis. Small panel in (b) shows C_{DN} beyond the scale at low wind speeds.

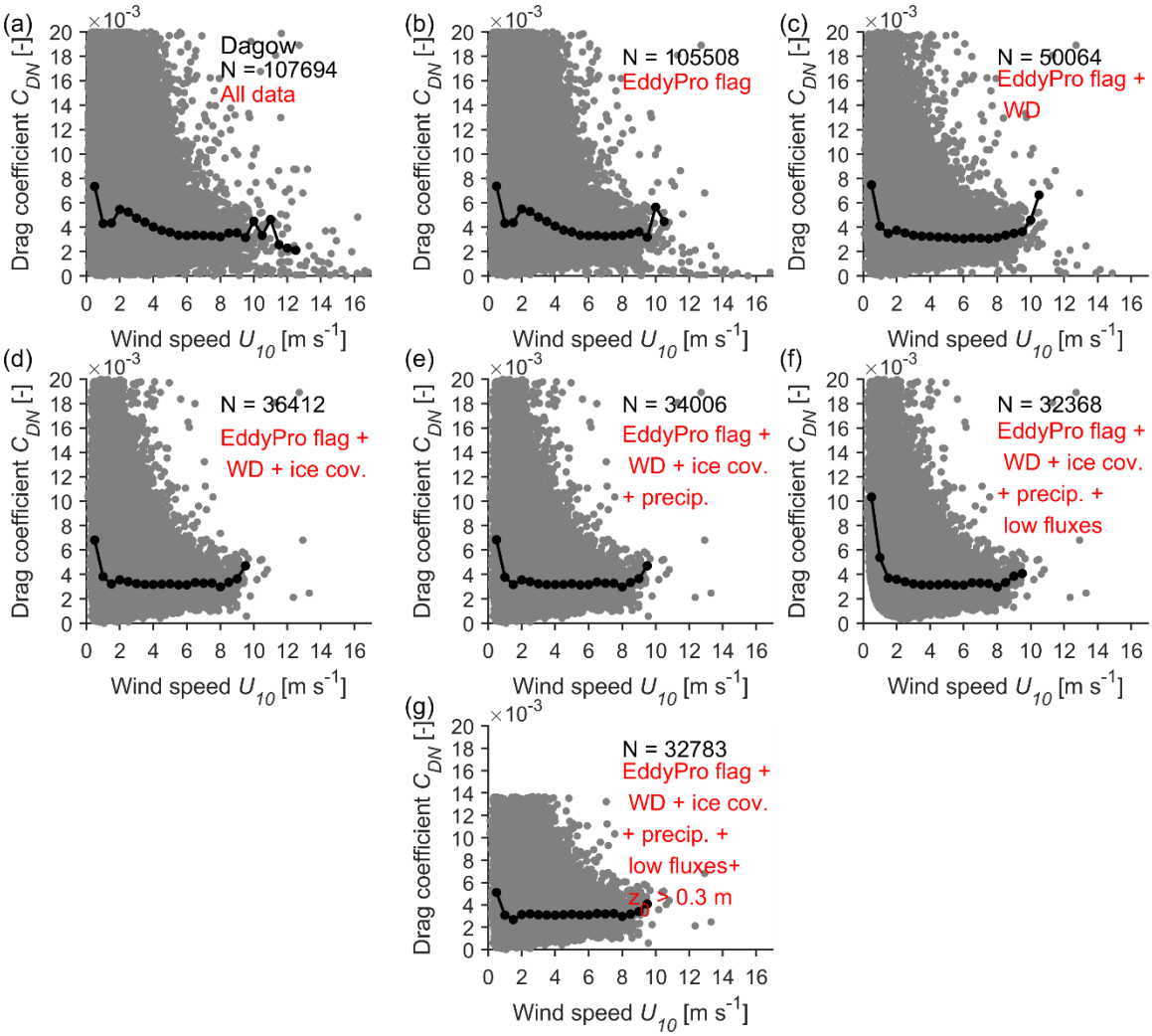

Figure S2. Effects of different steps of data filtering on estimated drag coefficients exemplified for the dataset from Lake Dagow (Germany). Neutral drag coefficients (C_{DN}) as a function of wind speed at 10 m height (U_{10}) are shown by grey dots that represent the estimates from individual 30 min flux measurements. The solid black line with circles shows logarithmic bin-averaged data in 0.5 m s^{-1} wind speed intervals. The number of data points (N) is indicated in the legend and a minimum of 10 data points was considered for bin-averaging. (a) No filtering was applied; (b) the data with quality flag equal to 2 indicating bad quality data (provided by EddyPro software, see details in Text S1) were removed; (c) wind directions (WD) were removed (60° < *WD* < 90°, 210° < *WD* < 270°), as the lake has an elongated shape, we considered the wind directions with the largest fetch; (d) the periods with ice cover were removed; (e) the periods with precipitation were removed; (f) low fluxes were removed ($u_* < 0.05$ m s^{-1}, $|H|, |E| < 10$ W m^{-2}); (g) removing the periods with surface roughness length $\boldsymbol{z_0 > 0.3}$ m.

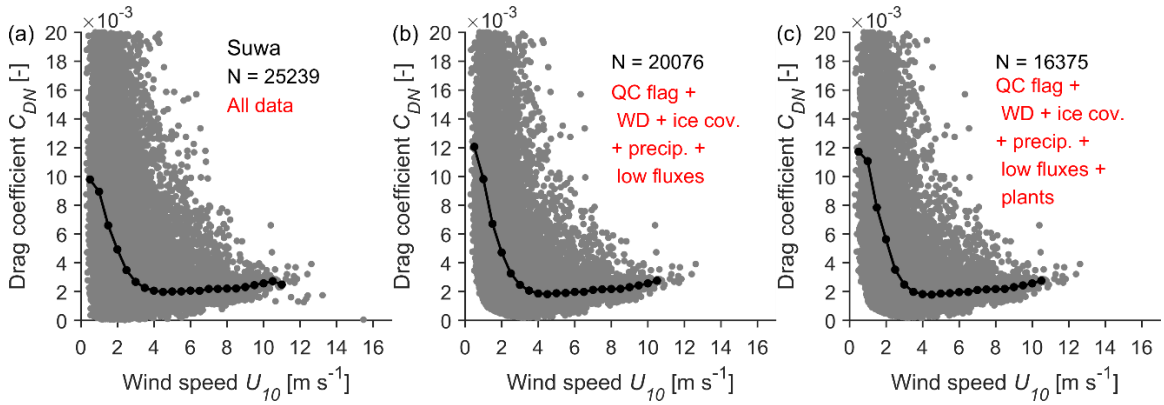

Figure S3. The effect of data filtering (similar to Figure S1): $\boldsymbol{C_{DN}}$ versus $\boldsymbol{U_{10}}$ for the dataset from Lake Suwa. (a) No filtering was applied; (b) all filters from Section 2.2 (except the periods with floating vegetation) were applied; (c) the periods with floating vegetation were removed (18.08.18-07.10.18; 15.05.19-09.09.19; 10.07.20-05.10.20).

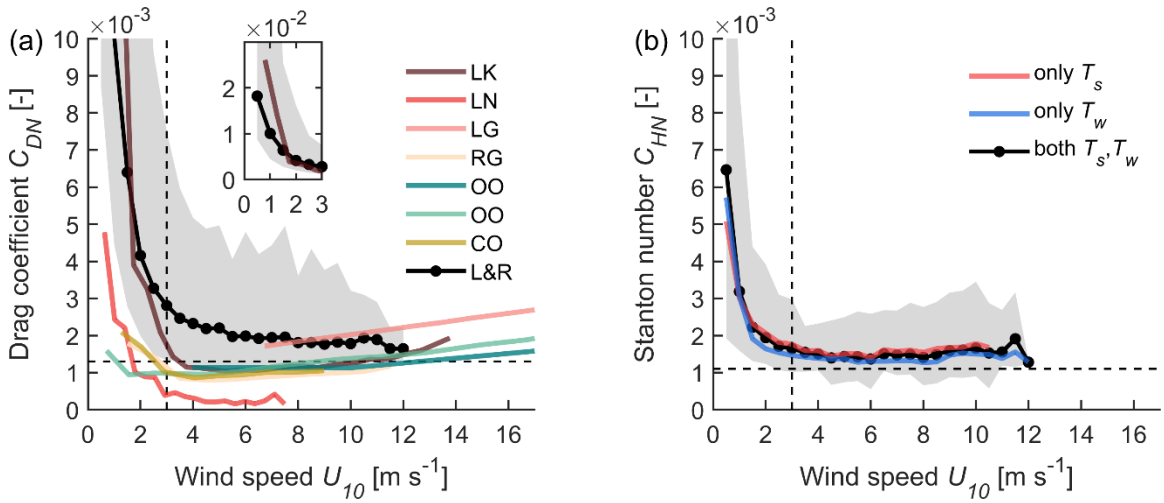

Figure S4. (a) $\boldsymbol{C_{DN}}$ versus $\boldsymbol{U_{10}}$. This panel is similar to Figure 2a except the fact that three additional lakes were excluded – Lake Quinghai (China), Nam Theun 2 Reservoir (Laos) and Bol'shoi Vilyui Lake (Russia). (b) Neutral Stanton number ($\boldsymbol{C_{HN}}$) versus $\boldsymbol{U_{10}}$. Three lines show bin averages of $\boldsymbol{C_{HN}}$ obtained using data with different measures of water temperature: skin

temperature $\boldsymbol{T_s}$ (red line), bulk water temperature $\boldsymbol{T_w}$ (blue line) or both (black line with circles). Shaded grey area in both panels indicates data between the 5th and 95th percentiles.

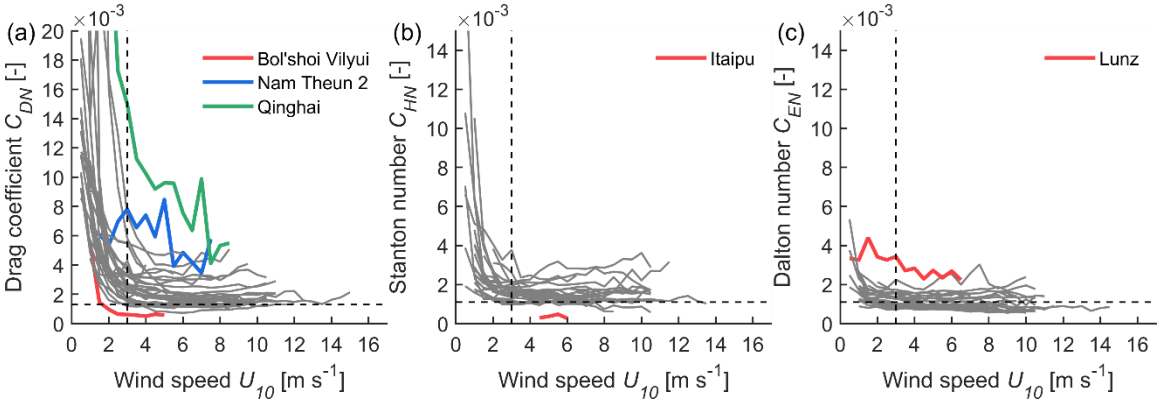

Figure S5. Neutral bin-averaged transfer coefficients (a) C_{DN}, (b) C_{HN}, (c) C_{EN} versus U_{10} are shown for all water bodies (grey lines). Thick colored lines (red, blue and green in (a) and red in (b) and (c)) show the water bodies which we marked as outliers, as their values were significantly larger or lower in comparison to other water bodies of similar size. Vertical and horizontal black dashed lines show a constant wind speed of 3 m s^{-1} and typical values of C_{DN}, C_{HN} = C_{EN} 1.3·10^{-3}, 1.1·10^{-3}, respectively. Note, the scale of Y-axis in (a) is different from (b) and (c) for better visibility.

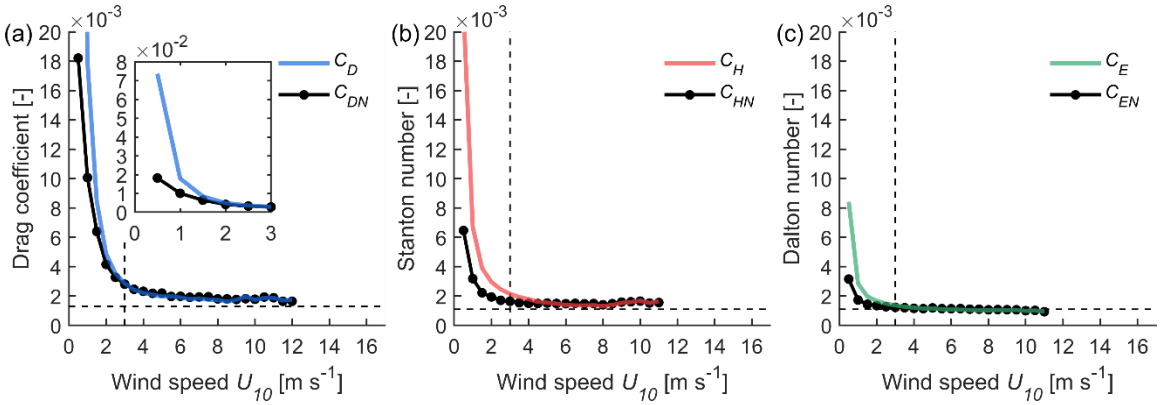

Figure S6. Comparison of the transfer coefficients (a) C_D, (b) C_H, (c) C_E (blue, red and green lines, respectively) with their counterparts adjusted for neutral atmospheric conditions C_{DN}, C_{HN}, C_{EN} (black line with circles) for bin-averaged values over all water bodies under study. Vertical and horizontal black dashed lines show a constant wind speed of 3 m s^{-1} and typical values of C_{DN}, C_{HN}= C_{EN} 1.3·10^{-3}, 1.1·10^{-3}, respectively. The smaller panel in (a) shows the drag coefficient for wind speeds less than 3 m s^{-1} at enlarged scale. It is apparent that atmospheric stability affected the transfer coefficients at low wind speeds only.

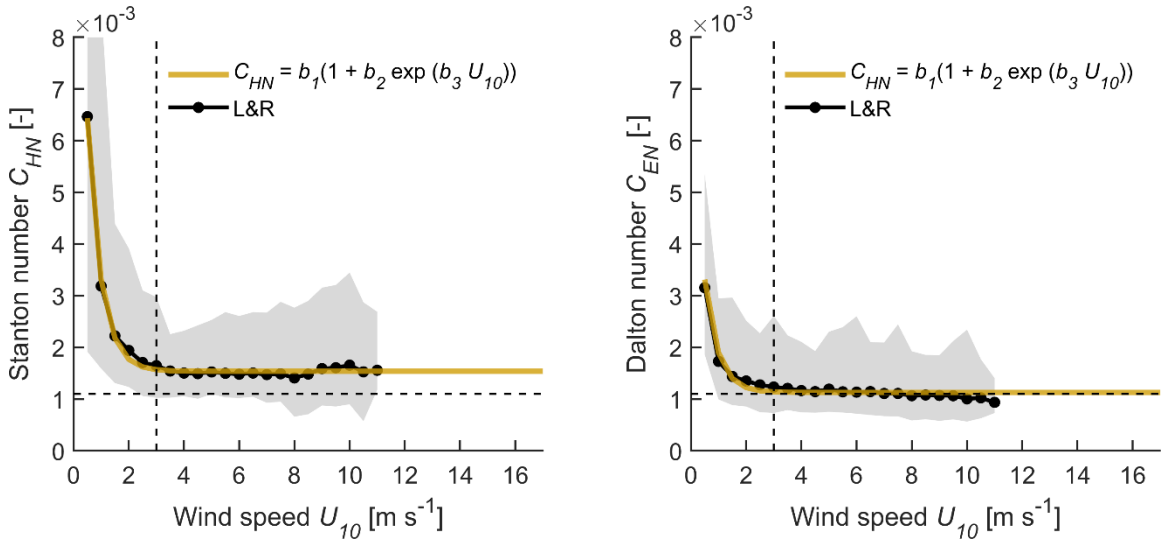

Figure S7. Neutral (a) Stanton number, (b) Dalton number marked by black line with symbols (similar to Figure 4a in the manuscript). The dark yellow line shows the function $C = b_1[1 + b_2\exp(b_3 U_{10})]$ proposed by Liu et al., (2020) with the fitted coefficients b_1 = 1.5·10^{-3}; b_2 = 8.8; b_3 = -2 for Stanton number and b_1 = 1.1·10^{-3}; b_2 = 5.5; b_3 = -2.1 for Dalton number (see details in Section 3.2). Vertical and horizontal black dashed lines show a constant wind speed of 3 m s^{-1} and typical value of $C_{HN} = C_{EN}$ being equal to 1.1·10^{-3}.

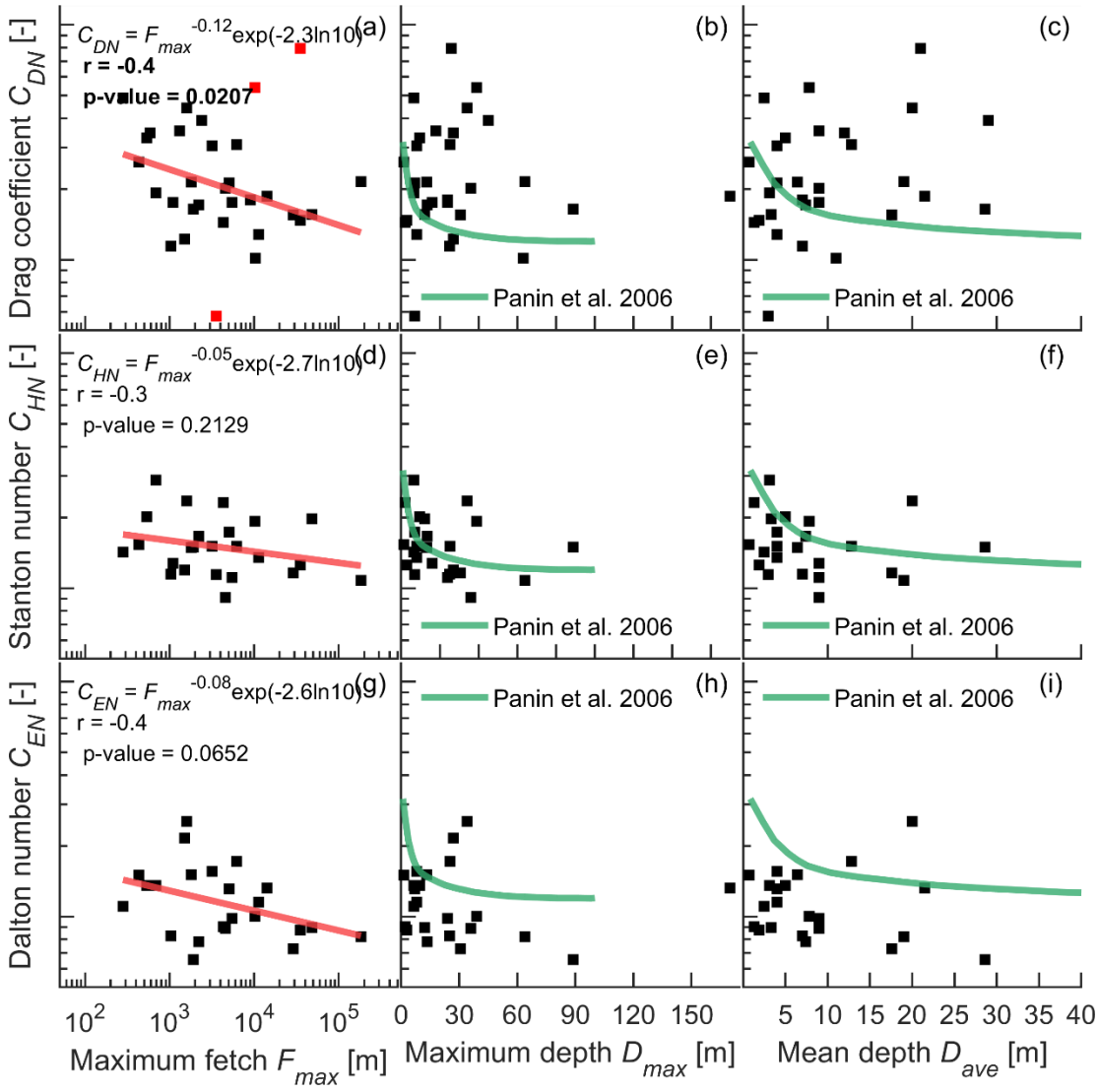

Figure S8. Mean neutral transfer coefficients (a, b, c) C_{DN}; (d, e, f) C_{HN}; (g, h, i) C_{EN} versus maximum fetch, maximum and average water depth of the water body. All plots show the exchange coefficients averaged for wind speeds exceeding 3 m s^{-1}. Each black square on the panels is the value of the transfer coefficient for one lake or reservoir. Red line in all plots shows linear regression in logarithmic domain ($\log_{10} y = A \log_{10} x + B$). The relationship between the transfer coefficients and selected lake characteristics is expressed as a power dependence $y = x^A \exp(B \ln 10)$, where A and B are the slope and intercept of the linear regression. Corresponding slope and intercept as well as the Pearson correlation coefficient and p-value are written at left upper corner of the plot. Three red squares in (a), (b) correspond to Lake Quinghai, Nam Theun 2 Reservoir and and Bol'shoi Vilyui Lake were not considered for linear regression analysis of the drag coefficient and the Pearson correlation for the drag coefficient. Green line illustrates the result from (Panin et al., 2006). There is a weak negative correlation between the Stanton and Dalton numbers and maximum fetch as well as a significant negative correlation between the drag coefficient and maximum fetch. No evidence for any kind of relationship between all transfer coefficients and maximum or average water depth was found.

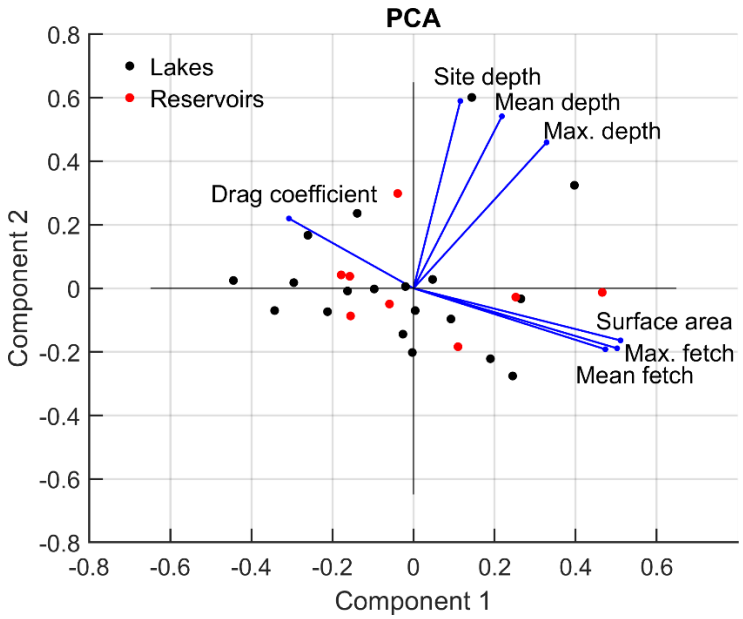

Figure S9. Principal component analysis for the data shown by black and red dots corresponding to the lakes and reservoirs, respectively. Representations of the original predictors in the first two principal component basis are presented with blue lines with dots. The fact that the drag coefficient and different types of the depths are nearly orthogonal to each other indicates that there is no correlation between them.

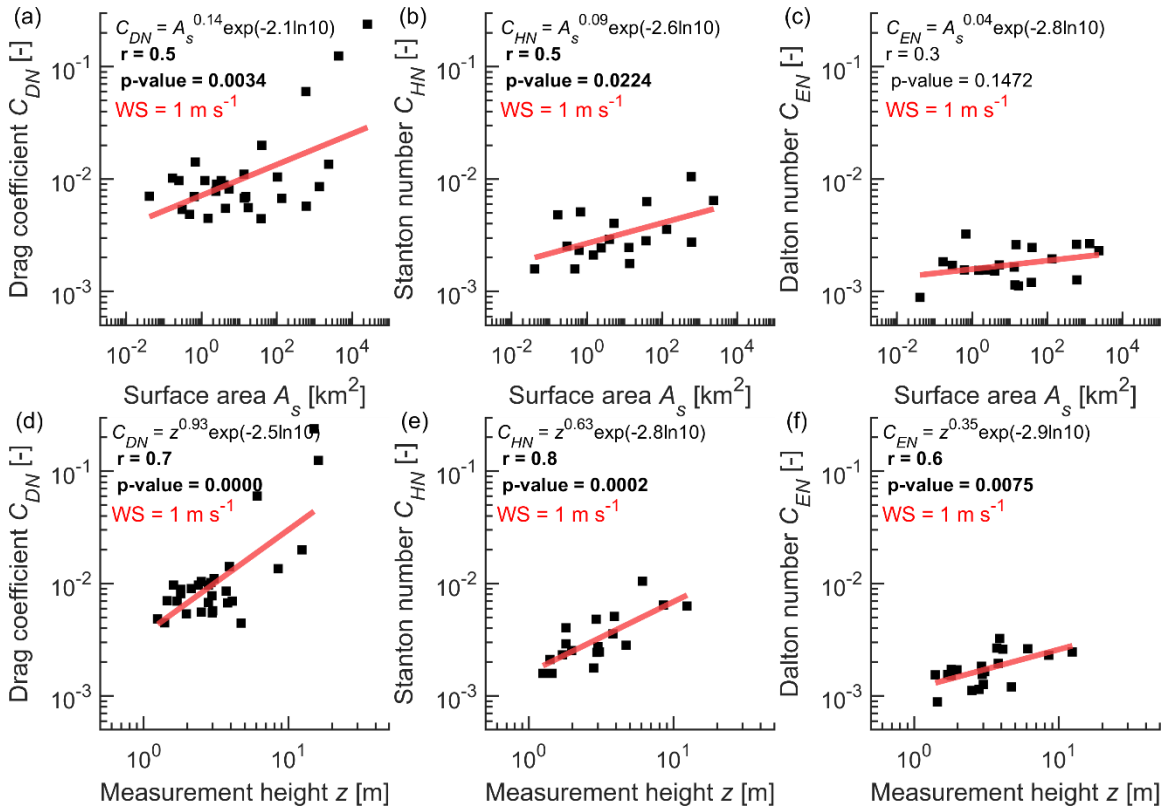

Figure S10. Mean neutral drag coefficient as a function of (a), (b), (c) lake surface area; (d), (e), (f) measurement height (if it changed – the average height for the measurement period was taken) at a fixed wind speed of 1 m s^{-1} (shown as "WS = 1 m s^{-1}"). Each black square on the panels represents the mean value of the drag coefficient for one lake or reservoir. Red line in all plots shows linear regression in logarithmic domain $\log_{10} y = A \log_{10} x + B$. The relationship between the transfer coefficients and selected lake characteristics is expressed as a power dependence $y = x^A \exp(B \ln 10)$, where A and B are the slope and intercept of the linear regression (shown in the upper left corner). Corresponding Pearson correlation coefficient and p-value are written at left upper corner of the plot. A significant positive correlation (marked by bold font) was found between C_{DN} , C_{HN} and surface area as well as measurement height (also C_{EN}).

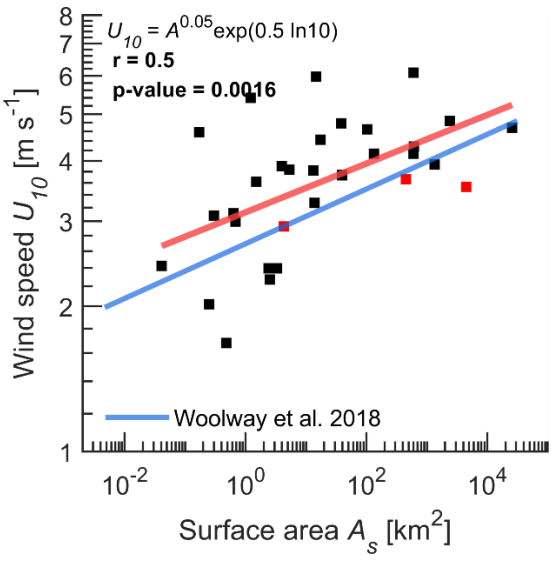

Figure S11. Relationship between the averaged wind speed estimated for all water bodies and the surface area. Red line in all plots shows linear regression in logarithmic domain. The blue line represents the results reported in (Woolway et al., 2018). The relationship between the wind speed and lake surface area is expressed as a power dependence written at left upper corner of the panel. The Pearson correlation coefficient and p-value are written at left upper corner of the panel. Three red squares correspond to Lake Quinghai, Nam Theun 2 Reservoir and and Bol'shoi Vilyui Lake but they were not excluded for this regression analysis.

Table S1. Lake and reservoirs under study and their characteristics. Corresponding datasets and information about their processing.

	Lake/Reservoir	Area A_s [km^2]	Mean/Max depth	Country	Filters	Accepted wind directions [°]	Publication	Data repository
1	Acton Lake (Reservoir)	0.12	- / 9.3	USA	QCF(2); WD; IC; LF	until 04.05.18: < 170; after: < 15 and > 300; > 130 and < 205	(Waldo et al., 2021)	(Waldo et al., 2021)
2	Lake Balaton	596	3.3 / 12.2	Hungary	QCF(≥ 6); LF	All	(Lükő et al., 2020, 2022)	https://zenodo.org/record/5597141#.YbIcK71_pPY
3	Bautzen Reservoir	5.3	7.4 / 13.5	Germany	WD; LF	> 195 and < 355	(Guseva et al., 2021)	***Data available from Uwe Spank
4	Bol'shoi Vilyui Lake	4.3	3 / 7	Russia	LF	All	(Stepanenko et al., 2018)	***Data available from Irina Repina
5	Lake Dagow	0.3	5 / 9.5	Germany	QCF(2); WD; IC; P; LF	> 60 and < 90; < 270 and > 210	(Guseva et al., 2021)	https://doi.org/10.18140/FLX/1669633
6	Daring Lake	14.8	- / 27	Canada	P; LF	* < 10 and > 270	(Golub et al., 2021)	(Golub et al., 2022)
7	Douglas Lake	13.7	9 / 24	USA	LF	* < 180 and > 270	(Morin et al., 2018; Golub et al., 2021)	
8	Eastmain Reservoir	602	11 / 63	Canada	WD; IC; P; LF	> 180 and < 330	(Demarty et al., 2011; Golub et al., 2021)	
9	Lake Erie	$2.6 \cdot 10^4$	19 / 64	USA	IC; P; LF	All	(Shao et al., 2015; Golub et al., 2021b)	
10	Itaipu Reservoir	$1.4 \cdot 10^3$	21.5 / 170	Brazil	WD; LF	< 30 and > 140	(Armani et al., 2020)	***Data available from Fernando Armani
11	Lake Klöntal	3.3	29 / 45	Switzerland	WD; LF	> 75 and < 243	(Sollberger et al., 2017)	***Data available from Werner Eugster
12	Lake Kuivajärvi	0.63	6.4 / 13.2	Finland	WD; P; LF	> 135 and < 185; > 315	(Heiskanen et al., 2015; Mammarella et al., 2015; Golub et al., 2021)	(Golub et al., 2022)
13	Lake Lunz	0.68	20 / 34	Austria	QCF(2); WD; IC; P; LF	> 195 and < 355	(Scholz et al., 2021)	https://doi.org/10.5281/zenodo.4519167
14	Lake Mendota	39.4	12.8/25.3	USA	WD; IC; P; LF	< 30; > 285		(Desai, 2018)
15	Nam Theun 2 Reservoir	450	7.8/39	Laos	P; LF; T	All	(Deshmukh et al., 2014)	(Golub et al., 2022)

16	Lake Ngoring	610.7	17.6/30.7	China	WD; LF	> 53 and < 175	(Han, 2020; Han et al., 2020)	https://dataverse.harvard.edu/dataset.xhtml?persistentId=doi:10.7910/DVN/SRIAYJ;
17	Lake Pallasjärvi	17.2	9/36	Finland	P; LF	* < 60 and > 180	(Lohila et al., 2015; Golub et al., 2021)	(Golub et al., 2022)
18	Lake Qinghai	$4.4 \cdot 10^3$	21/26	China	WD; LF	< 110 and > 325	(Li et al., 2016; Li et al., 2018)	https://data.tpdc.ac.cn/en/data/1df8f705-8a98-4ede-8de7-d065f7f674bd/
19	Rappbode Reservoir	4	28.6/89	Germany	WD; LF	> 180 and < 240	(Spank et al., 2020)	***Data available from Uwe Spank
20	Ross Barnett Reservoir	134	4/8	USA	P; LF	All	(Liu et al., 2009)	(Golub et al., 2022)
21	Lake Rotsee	0.48	9/16	Switzerland	WD; LF	> 7 and < 65; > 235 and < 262	(Schubert et al., 2012)	***Data available from Werner Eugster
22	Siberian Lake	1.21	3.1/6.5	Russia	QCF(2); IC; LF; T	All	(Franz et al., 2018)	***Data available from Torsten Sachs
23	Lake Soppensee	0.25	12/27	Switzerland	LF	All	(Eugster, 2003)	***Data available from Werner Eugster
24	Lake Suwa	13.3	4/6.9	Japan	QCF(≥ 6); WD; IC; LC; P; LF	< 5 and > 240	(Iwata et al., 2018, 2020)	http://asiaflux.net/index.php?page_id=1355
25	Lake Taihu	$2.4 \cdot 10^3$	1.9/3	China	QCF(2); LF	All *Data from PTS point only	(Zhang et al., 2020)	https://dataverse.harvard.edu/dataset.xhtml?persistentId=doi:10.7910/DVN/HEWCWM
26	Lake Tämnaren	38	1.3/2	Sweden	WD; IC; LF	> 120 and < 333	(Podgrajsek et al., 2014; Sahlée et al., 2014)	(Golub et al., 2022)
27	Lake Toolik	1.5	7/25	USA	P; LF	All	(Eugster et al., 2020; Golub et al., 2021)	
28	Lake Valkea Kotinen	$4.1 \cdot 10^{-2}$	2.5/-	Finland	WD; P; LF	> 134 and < 180; > 300 and < 350	(Nordbo et al., 2011; Golub et al., 2021)	
29	Lake Vanajavesi	103	7/24	Finland	IC; LF	All	(Salgado et al., 2016; Golub et al., 2021)	

30	Lake Villasjön	0.17	0.7/1.3	Sweden	WD; IC; LF	> 10 and < 75; > 114 and < 140	(Jammet et al., 2017; Jansen et al., 2019)	http://www.europe-fluxdata.eu/page21/site-details?id=SE-St1
31	Lake Wohlen (Reservoir)	2.5	9/18	Switzerland	WD;LF	> 245	(Eugster et al., 2011)	***Data available from Werner Eugster
*QCF(2 or ≥ 6): removing unacceptable data with quality check flags equal to 2 (EddyPro software,(LI-COR, Inc, 2021)) and ≥ 6 (Eddy-covariance software TK3,(Mauder & Foken, 2015)) (Foken et al., 2012); WD: limitation of the wind directions (site-specific); IC: removing periods with ice cover; P: removing periods with precipitation; LF: removing low fluxes ($\boldsymbol{u}_*$<0.05 m s^{-1}, $\lvert\boldsymbol{H}\rvert$, $\lvert\boldsymbol{E}\rvert$<10 W m^{-2}); L: removing periods with floating vegetation on the water surface (18.08.18-07.10.18; 15.05. 2019-09.09.2019; 10.07.20-05.10.20, Lake Suwa, Japan); T: removing periods with low water level (appearance of many small islands around the measurement location in Nam Theun 2 Reservoir) or removing periods when footprint was on the shore (Siberian Lake)								
* Wind directions were removed by the owners of the dataset.								

References

Armani, F. A. S., Dias, N. L., & Damázio, J. M. (2020). Eddy-covariance CO2 fluxes over Itaipu lake, southern Brazil. *RBRH*, *25*, e43. https://doi.org/10.1590/2318-0331.252020200060

Demarty, M., Bastien, J., & Tremblay, A. (2011). Annual follow-up of gross diffusive carbon dioxide and methane emissions from a boreal reservoir and two nearby lakes in Québec, Canada. *Biogeosciences*, *8*(1), 41–53. https://doi.org/10.5194/bg-8-41-2011

Desai, A. (2018). *AmeriFlux AmeriFlux US-Pnp Lake Mendota, Picnic Point Site* [Data set]. AmeriFlux; University of Wisconsin Madison. https://doi.org/10.17190/AMF/1433376

Deshmukh, C., Serça, D., Delon, C., Tardif, R., Demarty, M., Jarnot, C., Meyerfeld, Y., Chanudet, V., Guédant, P., Rode, W., Descloux, S., & Guérin, F. (2014). Physical controls on CH₄ emissions from a newly flooded subtropical freshwater hydroelectric reservoir: Nam Theun 2. *Biogeosciences*, *11*(15), 4251–4269. https://doi.org/10.5194/bg-11-4251-2014

Eugster, W. (2003). CO_2 exchange between air and water in an Arctic Alaskan and midlatitude Swiss lake: Importance of convective mixing. *Journal of Geophysical Research*, *108*(D12), 4362. https://doi.org/10.1029/2002JD002653

Eugster, W., DelSontro, T., Shaver, G. R., & Kling, G. W. (2020). Interannual, summer, and diel variability of CH_4 and CO_2 effluxes from Toolik Lake, Alaska, during the ice-free periods 2010–2015. *Environmental Science: Processes & Impacts*, 10.1039.D0EM00125B. https://doi.org/10.1039/D0EM00125B

Eugster, W., DelSontro, T., & Sobek, S. (2011). *Eddy covariance flux measurements confirm extreme CH₄ emissions from a Swiss hydropower reservoir and resolve their short-term variability* [Preprint]. Biogeochemistry: Greenhouse Gases. https://doi.org/10.5194/bgd-8-5019-2011

Foken, T., Leuning, R., Oncley, S. R., Mauder, M., & Aubinet, M. (2012). Corrections and Data Quality Control. In M. Aubinet, T. Vesala, & D. Papale (Eds.), *Eddy Covariance* (pp. 85–131). Springer Netherlands. https://doi.org/10.1007/978-94-007-2351-1_4

Franz, D., Mammarella, I., Boike, J., Kirillin, G., Vesala, T., Bornemann, N., Larmanou, E., Langer, M., & Sachs, T. (2018). Lake-Atmosphere Heat Flux Dynamics of a Thermokarst Lake in Arctic Siberia. *Journal of Geophysical Research: Atmospheres*, *123*(10), 5222–5239. https://doi.org/10.1029/2017JD027751

Golub, M., Desai, A. R., Vesala, T., Mammarella, I., Ojala, A., Bohrer, G., Weyhenmeyer, G. A., Blanken, P. D., Eugster, W., Koebsch, F., Chen, J., Czajkowski, K. P., Deshmukh, C., Guérin, F., Heiskanen, J. J., Humphreys, E. R., Jonsson, A., Karlsson, J., Kling, G. W., … Xiao, W. (2021a). *New insights into diel to interannual variation in carbon dioxide emissions from lakes and reservoirs* [Preprint]. Environmental Sciences. https://doi.org/10.1002/essoar.10507313.1

Golub, M., Desai, A. R., Vesala, T., Mammarella, I., Ojala, A., Bohrer, G., Weyhenmeyer, G. A., Blanken, P. D., Eugster, W., Koebsch, F., Chen, J., Czajkowski, K. P., Deshmukh, C., Guérin, F., Heiskanen, J. J., Humphreys, E. R., Jonsson, A., Karlsson, J., Kling, G. W., … Xiao, W. (2021b). *New insights into diel to interannual variation in carbon dioxide emissions from lakes and reservoirs* [Preprint]. Environmental Sciences. https://doi.org/10.1002/essoar.10507313.1

Golub, M., Desai, A. R., Vesala, T., Mammarella, I., Ojala, A., Bohrer, G., Weyhenmeyer, G., Blanken, P., Eugster, W., Franz, D., Koebsch, F., Chen, J., Czajkowski, K., Deshmukh, C. S., Elbers, J., Friborg, T., Glatzel, S., Guerin, F., Heiskanen, J., … Xiao, W. (2022). *Half-hourly gap-filled Northern Hemisphere lake and reservoir carbon flux and micrometeorology, 2006—2015* [Data set]. Environmental Data Initiative. https://doi.org/10.6073/PASTA/87A35CA843D8739D75882520C724E99E

Guseva, S., Casper, P., Sachs, T., Spank, U., & Lorke, A. (2021). Energy Flux Paths in Lakes and Reservoirs. *Water*, *13*(22), 3270. https://doi.org/10.3390/w13223270

Han, B. (2020). *Eddy covariance data in Ngoring Lake in Tibet from 2011 to 2013* [Data set]. Harvard Dataverse. https://doi.org/10.7910/DVN/SRIAYJ

Han, B., Meng, X., Yang, Q., Wu, R., Lv, S., Li, Z., Wang, X., Li, Y., & Yu, L. (2020). Connections Between Daily Surface Temperature Contrast and CO_2 Flux Over a Tibetan Lake: A Case Study of Ngoring Lake. *Journal of Geophysical Research: Atmospheres*, *125*(6). https://doi.org/10.1029/2019JD032277

Heiskanen, J. J., Mammarella, I., Ojala, A., Stepanenko, V., Erkkilä, K., Miettinen, H., Sandström, H., Eugster, W., Leppäranta, M., Järvinen, H., Vesala, T., & Nordbo, A. (2015). Effects of water clarity on lake stratification and lake-atmosphere heat exchange. *Journal of Geophysical Research: Atmospheres*, *120*(15), 7412–7428. https://doi.org/10.1002/2014JD022938

Iwata, H., Hirata, R., Takahashi, Y., Miyabara, Y., Itoh, M., & Iizuka, K. (2018). Partitioning Eddy-Covariance Methane Fluxes from a Shallow Lake into Diffusive and Ebullitive Fluxes. *Boundary-Layer Meteorology*, *169*(3), 413–428. https://doi.org/10.1007/s10546-018-0383-1

Iwata, H., Nakazawa, K., Sato, H., Itoh, M., Miyabara, Y., Hirata, R., Takahashi, Y., Tokida, T., & Endo, R. (2020). Temporal and spatial variations in methane emissions from the littoral zone of a shallow mid-latitude lake with steady methane bubble emission areas. *Agricultural and Forest Meteorology*, *295*, 108184. https://doi.org/10.1016/j.agrformet.2020.108184

Jammet, M., Dengel, S., Kettner, E., Parmentier, F.-J. W., Wik, M., Crill, P., & Friborg, T. (2017). Year-round CH₄ and CO₂ flux dynamics in two contrasting freshwater ecosystems of the subarctic. *Biogeosciences*, *14*(22), 5189–5216. https://doi.org/10.5194/bg-14-5189-2017

Jansen, J., Thornton, B. F., Jammet, M. M., Wik, M., Cortés, A., Friborg, T., MacIntyre, S., & Crill, P. M. (2019). Climate-Sensitive Controls on Large Spring Emissions of CH_4 and CO_2 From Northern Lakes. *Journal of Geophysical Research: Biogeosciences*, *124*(7), 2379–2399. https://doi.org/10.1029/2019JG005094

Li, X., Yang, X., Ma, Y., Hu, G., Hu, X., Wu, X., Wang, P., Huang, Y., Cui, B., & Wei, J. (2018). Qinghai Lake Basin Critical Zone Observatory on the Qinghai-Tibet Plateau. *Vadose Zone Journal*, *17*(1), 180069. https://doi.org/10.2136/vzj2018.04.0069

Li, X.-Y., Ma, Y.-J., Huang, Y.-M., Hu, X., Wu, X.-C., Wang, P., Li, G.-Y., Zhang, S.-Y., Wu, H.-W., Jiang, Z.-Y., Cui, B.-L., & Liu, L. (2016). Evaporation and surface energy budget over the largest high-altitude saline lake on the Qinghai-Tibet Plateau: WATER AND ENERGY FLUX OVER QINGHAI LAKE. *Journal of Geophysical Research: Atmospheres*, *121*(18), 10,470-10,485. https://doi.org/10.1002/2016JD025027

LI-COR, Inc. (2021). *EddyPro® Software (Version 7.0)*. LI-COR. https://www.licor.com/env/support/EddyPro/home.html

Liu, C., Li, Y., Gao, Z., Zhang, H., Wu, T., Lu, Y., & Zhang, X. (2020). Improvement of Drag Coefficient Calculation Under Near-Neutral Conditions in Light Winds Over land. *Journal of Geophysical Research: Atmospheres*, *125*(24). https://doi.org/10.1029/2020JD033472

Liu, H., Zhang, Y., Liu, S., Jiang, H., Sheng, L., & Williams, Q. L. (2009). Eddy covariance measurements of surface energy budget and evaporation in a cool season over southern open water in Mississippi. *Journal of Geophysical Research*, *114*(D4), D04110. https://doi.org/10.1029/2008JD010891

Lohila, A., Tuovinen, J. P., Hatakka, J., Aurela, M., Vuorenmaa, J., Haakana, M., & Laurila, T. (2015). *Carbon dioxide and energy fluxes over a northern boreal lake*. *20*(4), 474–488.

Lükő, G., Torma, P., Krámer, T., Weidinger, T., Vecenaj, Z., & Grisogono, B. (2020). Observation of wave-driven air–water turbulent momentum exchange in a large but fetch-limited shallow lake. *Advances in Science and Research*, *17*, 175–182. https://doi.org/10.5194/asr-17-175-2020

Lükő, G., Torma, P., & Weidinger, T. (2022). Intra-Seasonal and Intra-Annual Variation of the Latent Heat Flux Transfer Coefficient for a Freshwater Lake. *Atmosphere*, *13*(2), 352. https://doi.org/10.3390/atmos13020352

Mammarella, I., Nordbo, A., Rannik, Ü., Haapanala, S., Levula, J., Laakso, H., Ojala, A., Peltola, O., Heiskanen, J., Pumpanen, J., & Vesala, T. (2015). Carbon dioxide and energy fluxes over a small boreal lake in Southern Finland: CO_2 and Energy Fluxes Over Lake. *Journal of Geophysical Research: Biogeosciences*, *120*(7), 1296–1314. https://doi.org/10.1002/2014JG002873

Mauder, M., & Foken, T. (2015). *Eddy-Covariance Software TK3*. Zenodo. https://doi.org/10.5281/ZENODO.20349

Morin, T. H., Rey-Sánchez, A. C., Vogel, C. S., Matheny, A. M., Kenny, W. T., & Bohrer, G. (2018). Carbon dioxide emissions from an oligotrophic temperate lake: An eddy covariance approach. *Ecological Engineering*, *114*, 25–33. https://doi.org/10.1016/j.ecoleng.2017.05.005

Nordbo, A., Launiainen, S., Mammarella, I., Leppäranta, M., Huotari, J., Ojala, A., & Vesala, T. (2011). Long-term energy flux measurements and energy balance over a small boreal lake using eddy covariance technique. *Journal of Geophysical Research*, *116*(D2), D02119. https://doi.org/10.1029/2010JD014542

Panin, G. N., Nasonov, A. E., & Foken, T. (2006). Evaporation and heat exchange of a body of water with the atmosphere in a shallow zone. *Izvestiya, Atmospheric and Oceanic Physics*, *42*(3), 337–352. https://doi.org/10.1134/S0001433806030078

Podgrajsek, E., Sahlée, E., Bastviken, D., Holst, J., Lindroth, A., Tranvik, L., & Rutgersson, A. (2014). Comparison of floating chamber and eddy covariance measurements of lake greenhouse gas fluxes. *Biogeosciences*, *11*(15), 4225–4233. https://doi.org/10.5194/bg-11-4225-2014

Sahlée, E., Rutgersson, A., Podgrajsek, E., & Bergström, H. (2014). Influence from Surrounding Land on the Turbulence Measurements Above a Lake. *Boundary-Layer Meteorology*, *150*(2), 235–258. https://doi.org/10.1007/s10546-013-9868-0

Salgado, R., Potes, M., Mammarella, I., & Provenzale, M. (2016). *Measurements of Mass, Momentum and Energy fluxes over an ice/snow covered lake*. EGU.

Scholz, K., Ejarque, E., Hammerle, A., Kainz, M., Schelker, J., & Wohlfahrt, G. (2021). Atmospheric CO_2 Exchange of a Small Mountain Lake: Limitations of Eddy Covariance and Boundary Layer Modeling Methods in Complex Terrain. *Journal of Geophysical Research: Biogeosciences*, *126*(7). https://doi.org/10.1029/2021JG006286

Schubert, C. J., Diem, T., & Eugster, W. (2012). Methane Emissions from a Small Wind Shielded Lake Determined by Eddy Covariance, Flux Chambers, Anchored Funnels, and Boundary Model Calculations: A Comparison. *Environmental Science & Technology*, *46*(8), 4515–4522. https://doi.org/10.1021/es203465x

Shao, C., Chen, J., Stepien, C. A., Chu, H., Ouyang, Z., Bridgeman, T. B., Czajkowski, K. P., Becker, R. H., & John, R. (2015). Diurnal to annual changes in latent, sensible heat, and CO_2 fluxes over a Laurentian Great Lake: A case study in Western Lake Erie. *Journal of Geophysical Research: Biogeosciences*, *120*(8), 1587–1604. https://doi.org/10.1002/2015JG003025

Sollberger, S., Wehrli, B., Schubert, C. J., DelSontro, T., & Eugster, W. (2017). Minor methane emissions from an Alpine hydropower reservoir based on monitoring of diel and seasonal variability. *Environmental Science: Processes & Impacts*, *19*(10), 1278–1291. https://doi.org/10.1039/C7EM00232G

Spank, U., Hehn, M., Keller, P., Koschorreck, M., & Bernhofer, C. (2020). A Season of Eddy-Covariance Fluxes Above an Extensive Water Body Based on Observations from a Floating Platform. *Boundary-Layer Meteorology*, *174*(3), 433–464. https://doi.org/10.1007/s10546-019-00490-z

Stepanenko, V. M., Repina, I. A., Artamonov, A. Y., Gorin, S. L., Lykossov, V. N., & Kulyamin, D. V. (2018). Mid-depth temperature maximum in an estuarine lake. *Environmental Research Letters*, *13*(3), 035006. https://doi.org/10.1088/1748-9326/aaad75

Waldo, S., Beaulieu, J. J., Barnett, W., Balz, D. A., Vanni, M. J., Williamson, T., & Walker, J. T. (2021). Temporal trends in methane emissions from a small eutrophic reservoir: The key role of a spring burst. *Biogeosciences*, *18*(19), 5291–5311. https://doi.org/10.5194/bg-18-5291-2021

Woolway, R. I., Verburg, P., Lenters, J. D., Merchant, C. J., Hamilton, D. P., Brookes, J., Eyto, E., Kelly, S., Healey, N. C., Hook, S., Laas, A., Pierson, D., Rusak, J. A., Kuha, J., Karjalainen, J., Kallio, K., Lepistö, A., & Jones, I. D. (2018). Geographic and temporal variations in turbulent heat loss from lakes: A global analysis across 45 lakes. *Limnology and Oceanography*, *63*(6), 2436–2449. https://doi.org/10.1002/lno.10950

Zhang, Z., Zhang, M., Cao, C., Wang, W., Xiao, W., Xie, C., Chu, H., Wang, J., Zhao, J., Jia, L., Liu, Q., Huang, W., Zhang, W., Lu, Y., Xie, Y., Wang, Y., Pu, Y., Hu, Y., Chen, Z., … Lee, X. (2020). *A dataset of microclimate and radiation and energy fluxes from the Lake Taihu Eddy Flux Network* [Data set]. Harvard Dataverse. https://doi.org/10.7910/DVN/HEWCWM